JACS
JOURNAL OF THE AMERICAN CHEMICAL SOCIETY
pubs.acs.org/JACS
Article

An Accelerated Modular-Orthogonal Ni-Catalyzed Methodology to Symmetric and Nonsymmetric Constitutional Isomeric AB_2 to AB_9 Dendrons Exhibiting Unprecedented Self-Organizing Principles

Virgil Percec,* Shitao Wang, Ning Huang, Benjamin E. Partridge, Xuefeng Wang, Dipankar Sahoo, David J. Hoffman, Jagadeesh Malineni, Mihai Peterca, Ryan L. Jezorek, Na Zhang, Hina Daud, Paul D. Sung, Emily R. McClure, and Se Lin Song

Cite This: J. Am. Chem. Soc. 2021, 143, 17724–17743
Read Online
ACCESS | Metrics & More | Article Recommendations | Supporting Information

ABSTRACT: Five libraries of natural and synthetic phenolic acids containing five AB_3, ten constitutional isomeric AB_2, one AB_4, and one AB_5 were previously synthesized and reported by our laboratory in 5 to 11 steps. They were employed to construct seven libraries of self-assembling dendrons, by divergent generational, deconstruction, and combined approaches, enabling the discovery of a diversity of supramolecular assemblies including Frank–Kasper phases, soft quasicrystals, and complex helical organizations, some undergoing deracemization in the crystal state. However, higher substitution patterns within a single dendron were not accessible. Here we report three libraries consisting of 30 symmetric and nonsymmetric constitutional isomeric phenolic acids with unprecedented sequenced patterns, including two AB_2, three AB_3, eight AB_4, five AB_5, six AB_6, three AB_7, two AB_8, and one AB_9 synthesized by accelerated modular-orthogonal Ni-catalyzed borylation and cross-coupling. A single etherification step with 4-(*n*-dodecyloxy)benzyl chloride transformed all these phenolic acids, of interest also for other applications, into self-assembling dendrons. Despite this synthetic simplicity, they led to a diversity of unprecedented self-organizing principles: lamellar structures of interest for biological membrane mimics, helical columnar assemblies from rigid-solid angle dendrons forming Tobacco Mosaic Virus-like assemblies, columnar organizations from adaptable-solid angle dendrons forming disordered micellar-like nonhelical columns, columns from supramolecular spheres, five body-centered cubic phases displaying supramolecular orientational memory, rarely encountered in previous libraries forming predominantly Frank–Kasper phases, and two Frank–Kasper phases. Lessons from these self-organizing principles, discovered within a single generation of self-assembling dendrons, may help elaborate design principles for complex helical and nonhelical organizations of synthetic and biological matter.

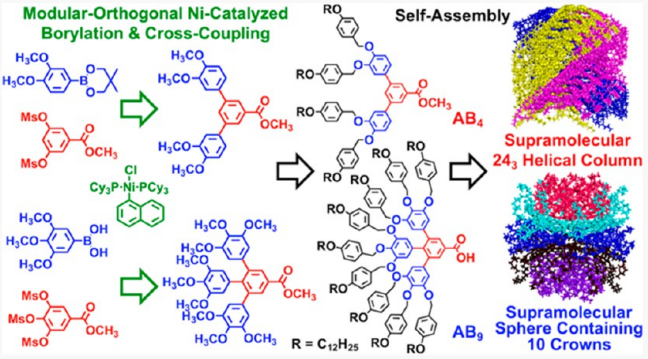

INTRODUCTION

Dendrimers and dendrons are branched, perfectly monodisperse macromolecules[1] prepared by iterative divergent,[2] convergent,[3] combined divergent-convergent,[4] and deconstruction[5] methodologies. They contain a predictable large number of chain ends[6] and smaller hydrodynamic volumes than those of the corresponding linear compounds.[7] These two features have facilitated a bridge between numerous disciplines including chemistry, physics, biology, nanomedicine, nanotechnology, and many others. De Gennes predicted a decrease in the reactivity of the functional groups on the periphery of dendrimers constructed by the divergent method.[8] This reactivity dependence on generation number was first observed during the divergent synthesis of the classic PAMAM dendrimers[2b,6] and subsequently during the divergent–convergent enlargement of dendronized polymers.[9] A complete self-interruption of their synthesis—that is, zero reactivity—was discovered by our laboratory in convergent,[10] divergent, and combined convergent–divergent[4] dendrimer synthesis as well as in the polymerization of self-assembling dendronized monomers.[11] Depending on their generation number, most dendrons and dendrimers are liquid or amorphous solids.[1,2] Our laboratory discovered simple strategies for the design of constitutional isomeric quasi-equivalent self-organizing dendrons, dendrimers, and dendron-

Received: August 12, 2021
Published: October 12, 2021

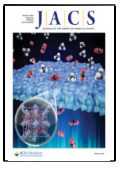

https://doi.org/10.1021/jacs.1c08502
J. Am. Chem. Soc. 2021, 143, 17724–17743

ized polymers that mimic the structure and function of simple biological systems, by combining chemically dissimilar units in their structure.[12] The history of this discovery was written by invitation.[13] This concept is related, but not identical, to the hydrophobic effect of proteins, nucleic acids, carbohydrates, and cell membranes, since it mediates self-assembly not only in water but also in organic solvents and in the bulk state. Related concepts evolved from many other laboratories.[14] The original self-assembling compounds were constructed from benzyl ether dendrons functionalized with aliphatic, fluorinated, semifluorinated, and oligooxyethylene fragments[12,15] and subsequently were expanded to other constructs to be discussed in more detail later. They led to the immediate discovery of helical self-organizations,[16] Frank−Kasper phases,[17] and soft quasicrystals[18] that were subsequently found in many other forms of soft matter such as block copolymers, lipids, surfactants, giant molecules, and DNA-grafted nanoparticles.[19−23] More recently they evolved in biological membrane mimics[24] and into a single component delivery system for mRNA.[25] The dream of self-organized complex soft matter is to reach the perfection of periodic arrays self-organized from inorganic materials[26] that are assembled from a small number of atoms as well as that of biological macromolecules that is self-organized from millions of atoms. Bridging between these two extreme size dimensions requires the elucidation of the mechanism of self-organization and the correlation with the molecular structure of their building blocks. Toward this goal our laboratory expanded self-assembling constitutional isomeric AB_2,[27a,c] AB_3,[27a,c] mixed AB_x−AB_y[27d] benzyl ether dendrons, dendrimers, and dendronized polymers[11b] into biphenyl-4-methyl ether,[27e] phenylpropyl ether,[27f] hybrid AB_4, AB_5 ethers,[27g] and biphenylpropyl ethers[5,27h] to discover, predict, and even organize a "nano-periodic table" of self-assembling dendrons.[27h] The principles elaborated with these libraries of self-assembling dendrons are valid for degrees of rotation mediated by a sequence of sp^2−sp^3−sp^3−sp^2 bonds for the benzyl ether and sp^2−sp^3−sp^3−sp^3−sp^3−sp^2 bonds for the phenylpropyl ether dendrons. We envisaged that the conformational freedom of self-assembling dendrons could be restricted by limiting their internal bonds to only sp^2−sp^2 bonds. However, until recently,[28] no methodology existed to access these structures in high yield for branching numbers above AB_3. Here we report the synthesis, self-assembly, and structural and retrostructural analysis of a new class of self-assembling dendrons based on *n*-phenylene units connected exclusively by sp^2−sp^2 bonds with branching numbers ranging from AB_2 to an unprecedented AB_9, many of them being constitutional isomers with defined-sequence. Their synthesis relies on natural polyphenols and phenolic acids as starting building blocks and an all Ni-catalyzed borylation and cross-coupling based on methodologies, including mixed-ligand, developed in our laboratory.[28]

RESULTS AND DISCUSSION

Selection and Synthesis of Precursors for the Modular-Orthogonal Preparation of Phenolic Acids. Four phenols and four phenolic acids (Figure 1), all of renewable natural origins,[29] were selected as starting materials for the modular-orthogonal synthesis of the new phenolic acids.

The four phenolic acids from Figure 1 were previously employed as starting building blocks in the synthesis of the constitutional isomeric AB_2 and AB_3 benzyl ether[10,11a,c,17a,27a,b] and phenylpropyl ether[27f] self-assembling dendrons. The four phenols from Figure 1 were used as starting building blocks in the synthesis of biphenyl-4-methyl (CEJ)[27g] and biphenyl-

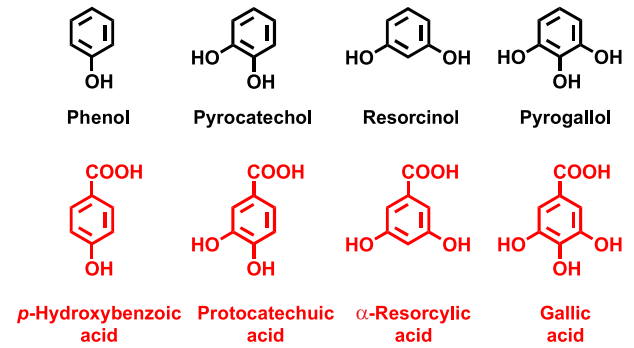

Figure 1. Natural phenols and phenolic acids employed in the synthesis of symmetric and nonsymmetric constitutional isomeric AB_2 to AB_9 phenolic acids.

Scheme 1. Synthesis of Boronic Ester and Boronic Acid Building Blocks[a]

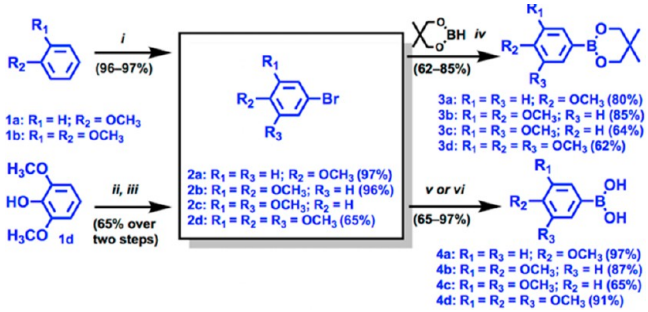

[a]Reagents and conditions: (*i*) NH_4Br, H_2O_2, AcOH, 23 °C, 4 h; (*ii*) NBS, NaH, MeOH, $CHCl_3$, − 60 to 23 °C, 2 h; (*iii*) $(CH_3O)_2SO_2$, NaOH, H_2O (reflux), 6 h; (*iv*) 10 mol % $NiCl_2$(dppp), 20 mol % dppf, Et_3N, toluene, 100 °C, 18 h; (*v*) (a) Mg, cat. I_2, THF (reflux), 40 min; (b) $B(OCH_3)_3$, −10 °C, 4 h; (c) HCl, 23 °C, 0.5 h; (*vi*) (a) *n*-BuLi, THF, −78 °C, 0.5 h; (b) $B(OCH_3)_3$, −78 °C, 4 h; (c) HCl, 23 °C, 0.5 h.

Scheme 2. Synthesis of Symmetric and Nonsymmetric Mesylated Building Blocks[a]

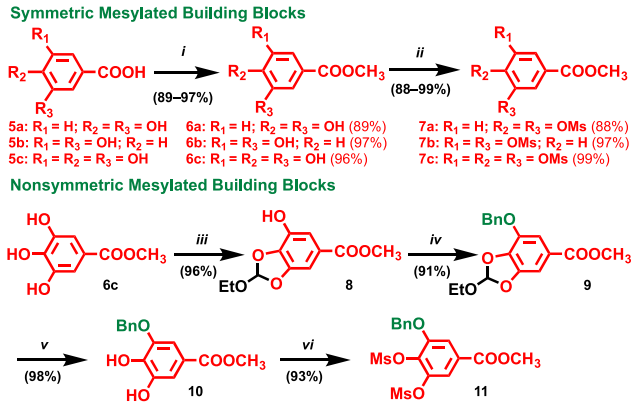

[a]Reagents and conditions: (*i*) cat. H_2SO_4, MeOH (reflux), 14 h; (*ii*) MsCl, pyridine, DCM, 0 to 23 °C, 5 h; (*iii*) $(EtO)_3CH$, Amberlyst 15, toluene (reflux), 16 h; (*iv*) BnCl, K_2CO_3, DMF, 120 °C, 12 h; (*v*) cat. HCl, MeOH, 23 °C, 0.5 h; (*vi*) MsCl, pyridine, DCM, 0 to 23 °C, 16 h.

https://doi.org/10.1021/jacs.1c08502
J. Am. Chem. Soc. 2021, 143, 17724−17743

Table 1. Synthesis of Symmetric Constitutional Isomeric, Sequence-Defined AB_2 to AB_9 Permethylated Phenolic Esters

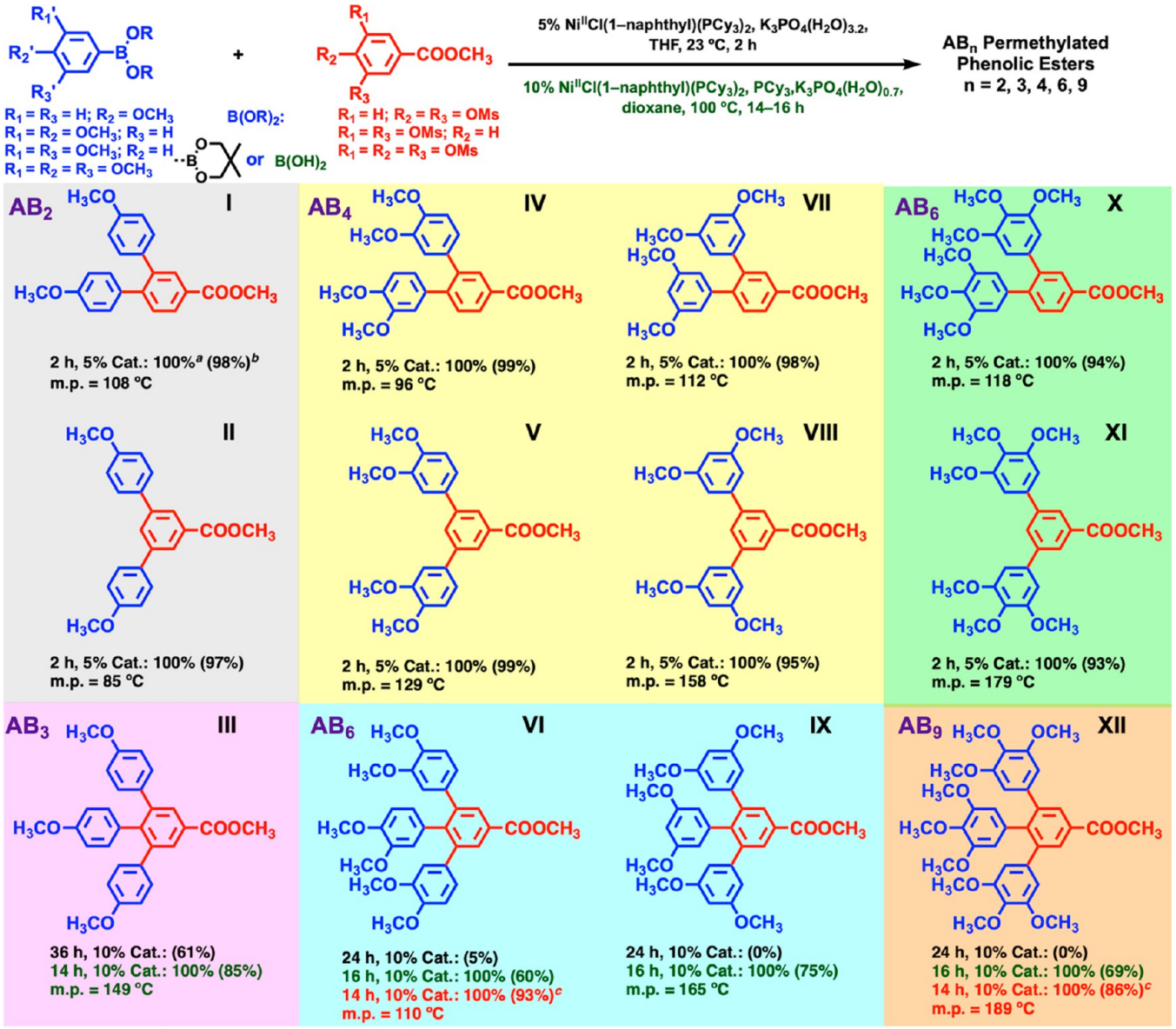

[a]Conversion. [b]Isolated yield. [c]Yield by nonsymmetric method.

propyl ether[5,27h] self-assembling dendrons. In the current synthetic methodology, the phenol group can provide both the aryl mesylate electrophile for the borylation reaction[28e,f] and the corresponding borylate or boronic acid nucleophiles; all of them are required in the Ni-catalyzed Suzuki–Miyaura cross-coupling reaction (Scheme 1). Therefore, they are orthogonal functional groups.

4-Methoxy- and 3,4-dimethoxy-1-bromobenzene (**2a**, **2b**) (Scheme 1) were synthesized by the bromination of veratrole and anisole in 97% and 98% yield, respectively, with NH_4Br/H_2O_2 in CH_3COOH.[30] 3,5-Dimethoxy-1-bromobenzene is commercially available and was used as received. 2,6-Dimethoxyphenol was brominated with *N*-bromosuccinimide (NBS) after deprotonation with NaH in a mixture of $CHCl_3$ and MeOH,[31] followed by methylation with Me_2SO_4 in acetone to generate 3,4,5-trimethoxy-1-bromobenzene (65%). Compounds **3a** to **3d** were prepared by the Ni-catalyzed borylation of **2a** to **2d** in 62% to 85% isolated yield with the mixed ligand dppp/dppf according to procedures elaborated in our laboratory.[28c,d] The boronic acids **4a** to **4d** were prepared from the corresponding aryl bromides **2a** to **2d** in 65% to 97% yield by conventional aryl Grignard or lithium methodologies (Scheme 1). Scheme 2 outlines the synthesis of the mesylated compounds **7a–c**. They were obtained in 88% to 99% yield starting from **6a–c** that were obtained by the esterification of the corresponding phenolic acids **5a–c** in 89% to 97% yield. Detailed procedures are available in the SI.

Accelerated Synthesis of Constitutional Isomeric, Sequence-Defined, Symmetric AB_2, AB_3, AB_4, AB_6, and AB_9 Permethylated Phenolic Esters. The Ni-catalyzed Suzuki–Miyaura cross-coupling of the multifunctional boronic esters **3a–d** and boronic acid aryl nucleophiles **4a–d** from Scheme 1 with the aryl electrophiles **7a–c** from Scheme 2 was performed with the σ-$Ni^{II}Cl(1\text{-naphthyl})(PCy_3)_2$ catalytic system with $K_3PO_4(H_2O)_{3.2}$ or $K_3PO_4(H_2O)_{0.7}$ as base in the absence or presence of excess PCy_3. This catalyst was

https://doi.org/10.1021/jacs.1c08502
J. Am. Chem. Soc. 2021, 143, 17724–17743

Scheme 3. Synthesis of Protected Constitutional Isomeric Nonsymmetric Permethylated Phenolic Esters and Protected Mesylated Building Blocks

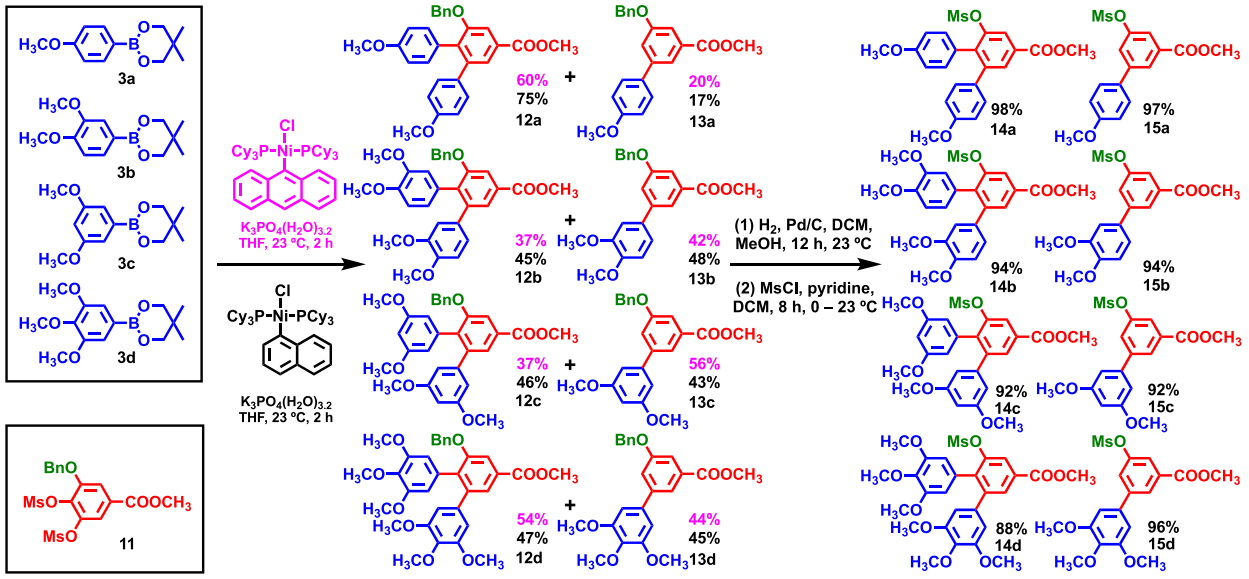

developed in our laboratory[28h] and provides quantitative cross-coupling reactions at room temperature (23 °C) for sterically nonhindered aryl electrophiles.

The aryl mesylates **7a** and **7b** from Scheme 2 cross-couple with the boronic esters **3a−d** from Scheme 1 with 100% conversion and 93 to 99% isolated yields in THF at room temperature in 2 h to produce eight permethylated phenolic esters (Table 1): two constitutional isomeric AB_2 (**I** and **II**, gray box), four constitutional isomeric AB_4 (**IV**, **V**, **VII**, **VII**, yellow box), and the two constitutional isomeric AB_6 (**X**, **XI**, green box). Under the same reaction conditions, the aryl mesylate **7c** from Scheme 2 provided maximum 61% isolated yield of the AB_3 (**III**, pink color), while the AB_6 (**VI**) was obtained in only 5% isolated yield. No reaction was observed in attempts to synthesize the AB_6 (**IX**) and the AB_9 (**XII**) in 24 h reaction time. Reducing the amount of water, *n*, in the K_3PO_4 base from 3.2 to 0.7, changing the aryl nucleophile from boronic ester to the more reactive boronic acid,[28g] increasing the reaction temperature to 100 °C (see green reaction conditions in Table 1) and using a reaction time of 14−16 h produced 100% conversion although only 85% to 60% isolated yields for **III**, **VI**, **IX**, and **XII** (Table 1). Compounds **VI** and **XII** were also obtained with 100% conversion and 93% to 86% isolated yields by a nonsymmetric method to be discussed later. It is important to mention that, despite its very high activity, the *σ*-catalyst $Ni^{II}Cl(1\text{-naphthyl})(PCy_3)_2$ is air stable since it enters the catalytic cycle of the cross-coupling at a different step from conventional Ni(II) catalysts.[28h] The synthesis of all compounds from Table 1 was also performed with precursors to this catalyst[28f,k] but with much lower conversion at longer reaction times.

All methyl ethers of the constitutional isomeric phenolic esters from Table 1 were quantitatively demethylated with BBr_3 in CH_2Cl_2 to provide the corresponding phenolic esters $\mathbf{I}_p$ to $\mathbf{XII}_p$ (Table S1). They were isolated in 78% to 99% yields.

Accelerated Synthesis of Constitutional Isomeric, Sequence-Defined, Nonsymmetric AB_4, AB_5, AB_6, AB_7, and AB_8 Phenolic Esters. The dimesylate **7a** undergoes cross-coupling with 100% conversion under mild conditions while the trimesylate **7c** does not (Table 1). Therefore, we protected the 3-position of **6c** to give benzyl ether **10** that was subsequently converted to the dimesylate **11**, *via* the two-step process illustrated in Scheme 2. This protection involved the modification of a previously developed method[32] to protect **6c**. The resulting **11** was cross-coupled with **3a−d** both in the presence of $Ni^{II}Cl(1\text{-naphthyl})(PCy_3)_2$ and in the presence of $Ni^{II}Cl(9\text{-anthracenyl})(PCy_3)_2$[28h] with $K_3PO_4(H_2O)_{3.2}$ as base. Surprisingly, two series of cross-coupled products were isolated from this reaction (Scheme 3).

A first series that is completely cross-coupled at the 4- and 5-mesylate positions yielded, depending on the structure of the catalyst and of the boronic ester employed, compounds **12a** (60%, 76%), **12b** (37%, 45%), **12c** (37%, 46%), and **12d** (54%, 47%). The second series of compounds—**13a** (20% 17%), **13b** (42%, 48%), **13c** (56%, 43%), and **13d** (44%, 45%)—were products most likely resulting from the reductive demesylation of **11** at the 4-position. These two series of compounds were obtained in high enough yields to permit their 3-benzyl ether deprotection by hydrogenolysis followed by mesylation of their 3-phenol position to generate two new series of starting building blocks, **14a−d** and **15a−d**, that were used for the synthesis of nonsymmetric constitutional isomeric phenolic acid derivatives. This reductive demesylation step raised mechanistic questions that will not be addressed in this study. Table 2 summarizes the synthesis of two constitutionally isomeric AB_4 (**XIII**, **XIV**, colored in yellow), AB_5 (**XV**, **XVIII**, **XXI**, colored in dark blue), AB_6 (**XVII**, **XX**, colored in light blue), AB_7 (**XVI**, **XIX**, **XXII**, colored in dark brown), and AB_8 (**XXIII**, **XXIV**, colored in light brown) nonsymmetric constitutional isomeric permethylated phenolic acids. They were realized via the cross-coupling of the mesylates **14a−d** with aryl boronic acids **4a−d**. The green reaction conditions (Table 2) involving dioxane as solvent at 100 °C and a 14 to 16 h reaction time provided 100% conversion with 72% to 97% isolated yields when $Ni^{II}Cl(1\text{-naphthyl})(PCy_3)_2$, $K_3PO_4(H_2O)_{0.7}$ was used as catalyst. All methyl ethers of the constitutional isomeric phenolic esters from Table 2 were

https://doi.org/10.1021/jacs.1c08502
J. Am. Chem. Soc. 2021, 143, 17724−17743

Table 2. Synthesis of Nonsymmetric Constitutional Isomeric, Sequence-Defined AB_4 to AB_8 Permethylated Phenolic Esters

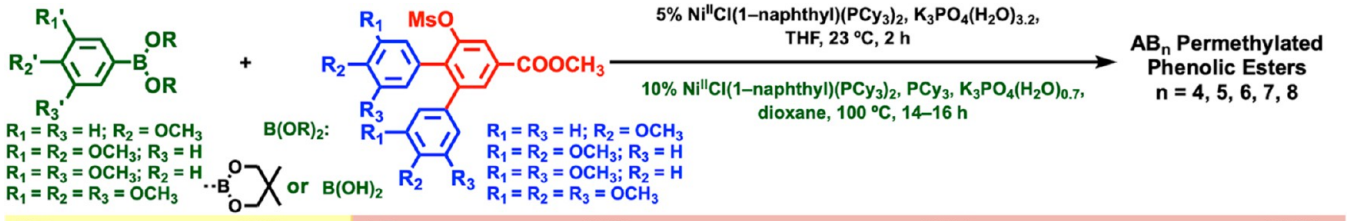

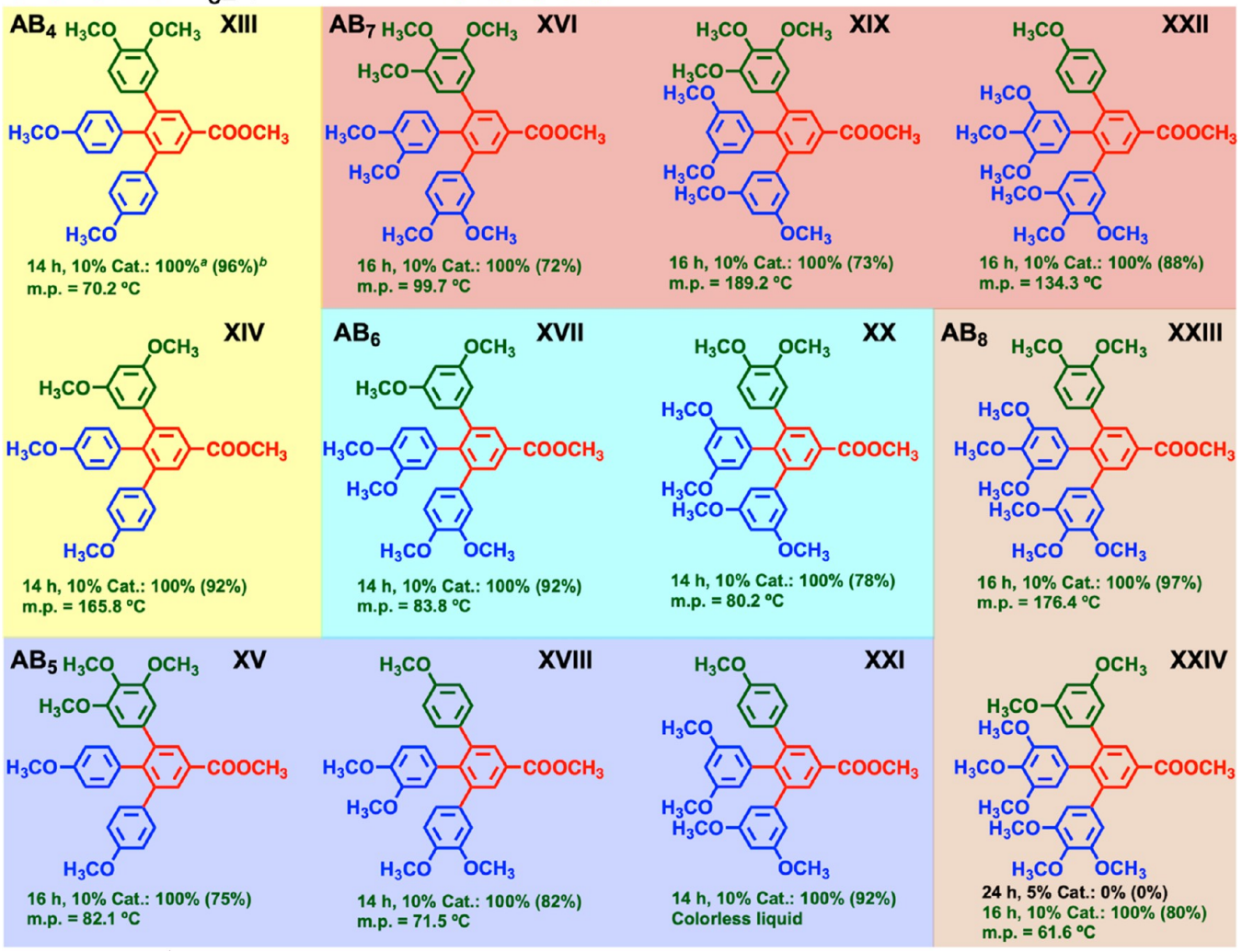

[a]Conversion. [b]Isolated yield.

quantitatively demethylated with BBr_3 in CH_2Cl_2 to provide the corresponding phenolic esters **XIII**$_p$ to **XXIV**$_p$ (Table S2). They were isolated in 69% to 96% yields.

Accelerated Synthesis of Constitutional Isomeric, Sequence-Defined, Nonsymmetric AB_3, AB_4, and AB_5 Phenolic Esters. The cross-coupling of the less sterically hindered nonsymmetric aryl mesylates **15a–d** from Scheme 3 was accomplished with the boronic esters **3a–d** at room temperature in THF with 100% conversion and 75% to 95% isolated yields in 2 h with the least active catalyst $Ni^{II}Cl(1\text{-naphthyl})(PCy_3)_2$, $K_3PO_4(H_2O)_{3.2}$, to provide the constitutionally isomeric AB_3 (**XXV**, **XXVI**, colored in magenta), AB_4 (**XXVII**, **XXVIII**, colored in yellow), and AB_5 (**XXIX**, **XXX**, colored in blue) (Table 3). All methyl ethers of the constitutional isomeric phenolic esters from Table 3 were quantitatively demethylated with BBr_3[33] in CH_2Cl_2 to provide the corresponding phenolic esters **XXVp** to **XXXp** (Table S3). They were isolated in 82% to 98% isolated yields.

One-Step Synthesis and Structural and Retrostructural Analysis of Constitutional Isomeric Symmetric Supramolecular Dendrimers Based on AB_2, AB_3, AB_4, AB_6, and AB_9 Dendrons. All phenolic esters **I**$_p$ to **XXX**$_p$ were etherified with 4-(*n*-dodecyloxy)benzyl chloride in DMF by using K_2CO_3 as base at 60 °C to provide the corresponding self-assembling dendrons **I**$_d$ to **XXX**$_d$ (Table 4). The etherification process was monitored by a combination of TLC, NMR, HPLC, and MALDI-TOF and reached completion in a maximum of 16 h. For selected compounds, the ester group from the apex of the dendron was transformed by basic hydrolysis into −COOH and by reduction with $LiAlH_4$ into $-CH_2OH$. The most surprising result was that after purification by column chromatography on silica gel with

https://doi.org/10.1021/jacs.1c08502
J. Am. Chem. Soc. 2021, 143, 17724–17743

Table 3. Synthesis of Nonsymmetric Constitutional Isomeric, Sequence-Defined AB_3 to AB_5 Permethylated Phenolic Esters

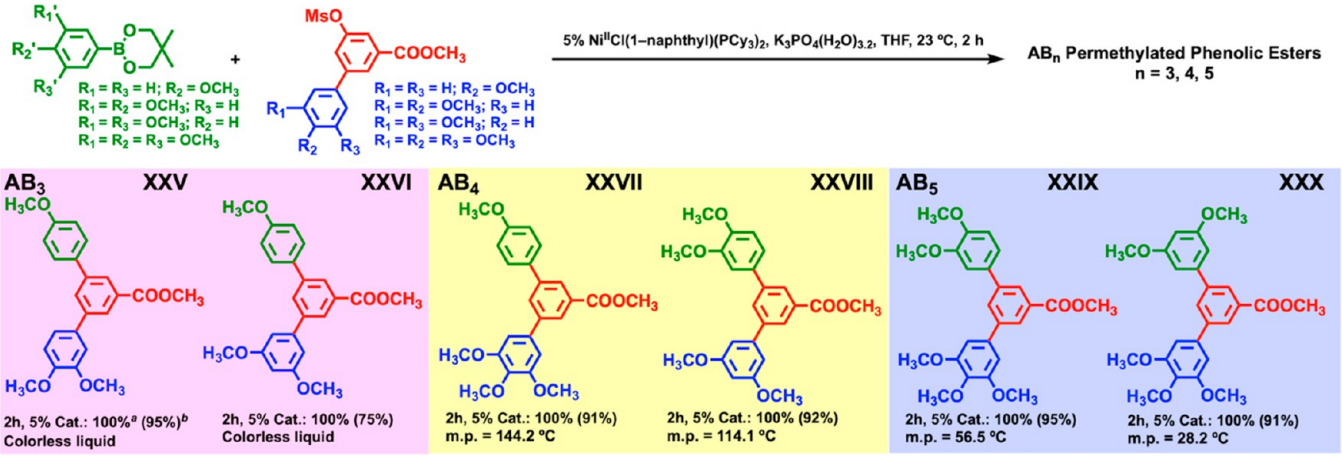

[a]Conversion. [b]Isolated yield.

ethyl acetate/hexane gradient as eluent, it was found, by a combination of DSC and X-ray diffraction, that all dendrons were self-organized into supramolecular dendrimers regardless of the functional group at their apex. This is a remarkable result since most of the previously synthesized self-assembling dendrons[5,10,11,15,27] required either a higher generation and/or a combination of an H-bonding or other molecular receptor at their apex and a higher generation to undergo self-assembly.

Table 4 summarizes the structural and retrostructural analysis of all self-assembling dendrons obtained from the constitutional isomeric, sequence-defined, symmetric supramolecular dendrimers based on AB_2, AB_3, AB_4, AB_6, and AB_9 dendrons. This was performed by the methodology elaborated in our laboratory involving a minimum combination of methods including DSC, X-ray diffraction experiments performed on powders and aligned fibers, helical diffraction theory[34] combined with experimental density experiments, molecular modeling, and reconstruction of the molecular models until the experimental XRD pattern agrees with the one of the model reconstructed by Cerius 2 software.[35] Their DSC traces are shown in Figures S1, S2, and S3 while representative small and wide-angle X-ray scattering (SAXS and WAXS) experiments on oriented fibers[34b] will be discussed later. A remarkable conclusion comes from a brief inspection of Table 4. Both AB_2 ($\mathbf{I}_d$ and $\mathbf{II}_d$) and AB_3 ($\mathbf{III}_d$) constitutional isomers and one of the four constitutional isomeric AB_4 ($\mathbf{VIII}_d$) exhibit lamellar phases. This represents 33% out of the 12 molecules from Table 4 and is considered to be an unusually large fraction. Surprisingly the AB_2 ($\mathbf{I}_d$) and the AB_3 ($\mathbf{III}_d$) exhibit lamellar assemblies while in the corresponding benzyl ethers they form only helical columnar self-organizations.[27c] The second unexpected result is that two constitutional isomeric AB_4 ($\mathbf{V}_d$ with X = $-CO_2CH_3$, $-CH_2OH$, $-COOH$, and $\mathbf{VII}_d$ with X = $-CO_2CH_3$), four constitutional isomeric AB_6 ($\mathbf{VI}_d$ with X = $-CO_2CH_3$, $-CH_2OH$, COOH, $\mathbf{IX}_d$ with X = $-CO_2CH_3$, $\mathbf{X}_d$ with X = $-CO_2CH_3$, $-CH_2OH$, and $\mathbf{XI}_d$ with X = $-CO_2CH_3$, $-CH_2OH$, $-COOH$), and the AB_9 ($\mathbf{XII}_d$ with X = CO_2CH_3, $-CH_2OH$) exhibit columnar assemblies while in all other previous systems they formed spherical Frank–Kasper self-organizations.[5,10,11,15,27,35] They represent 58% of all molecules in Table 4. However, the most surprising observation comes from comparing the spherical assemblies formed by AB_4 ($\mathbf{IV}_d$ with X = $-CO_2CH_3$, $-CH_2OH$, $-COOH$), AB_6 ($\mathbf{X}_d$ with X = $-COOH$), and AB_9 ($\mathbf{XII}_d$ with X = $-COOH$). The last, AB_9, exhibits only the rarely encountered body centered cubic phase (BCC) while the first two (AB_4 and AB_6) self-organize into the most often encountered Frank–Kasper A15 ($Pm3n$) and σ ($P4_2/mnm$) phases. In this series of experiments BCC represents 33% of all spherical assemblies reported in Table 4. This result would not have been predicted when considering the trend observed in all previous libraries[5,10,11,15,27,35] and the theoretical work reported from several laboratories[36] although the title of ref 36b "Maximizing entropy by minimizing area: towards a new principle of self-organization" may indicate that a certain ratio between the sp^3–sp^3 and sp^2–sp^2 bonds may not allow the entropy increase required by self-organization in Frank–Kasper phases.

Therefore, this library raises the fundamental question: why are these self-assembling dendrons so different from the previously reported libraries? Is it due to the lack of sp^3–sp^3 bonds from benzyl ethers and other ethers? Are they more stable than those from previous libraries and cannot generate two different kinds of spheres as required by the A15 Frank–Kasper phase?[17] However, the definitive answer to this question, which is very fundamental to the field of self-organization and will be answered with the building blocks reported here, is outside the scope of this study. Another remarkable result was provided by the self-assembling dendron $\mathbf{V}_d$ with X = $-CO_2CH_3$, the less ordered $\mathbf{V}_d$ with X = $-CH_2OH$, and the disordered $\mathbf{V}_d$ with X = $-COOH$ from Table 4. $\mathbf{V}_d$ with X = $-CO_2CH_3$ self-organizes into a highly ordered helical column by principles resembling those of tobacco mosaic virus (TMV).[11b,16,17] This self-assembly process will be discussed in a different subchapter together with the mechanisms of lamellar and BCC self-organizations.

One-Step Synthesis and Structural and Retrostructural Analysis of Constitutional Isomeric, Sequence-Defined, Nonsymmetric Supramolecular Dendrimers Based on AB_3, AB_4, AB_5, AB_6, AB_7, and AB_8 Dendrons. Nonsymmetric self-assembling dendrons were not investigated and reported in the previous libraries,[27] as their synthesis would have required multiple iterative protective-deprotection steps and a substantial increase of the number of synthetic steps.

https://doi.org/10.1021/jacs.1c08502
J. Am. Chem. Soc. 2021, 143, 17724–17743

Table 4. Structural and Retrostructural Analysis of Supramolecular Dendrimers Self-Assembled from the Library of Symmetric Constitutional Isomeric AB_2 to AB_9 Self-Assembling Dendrons[a]

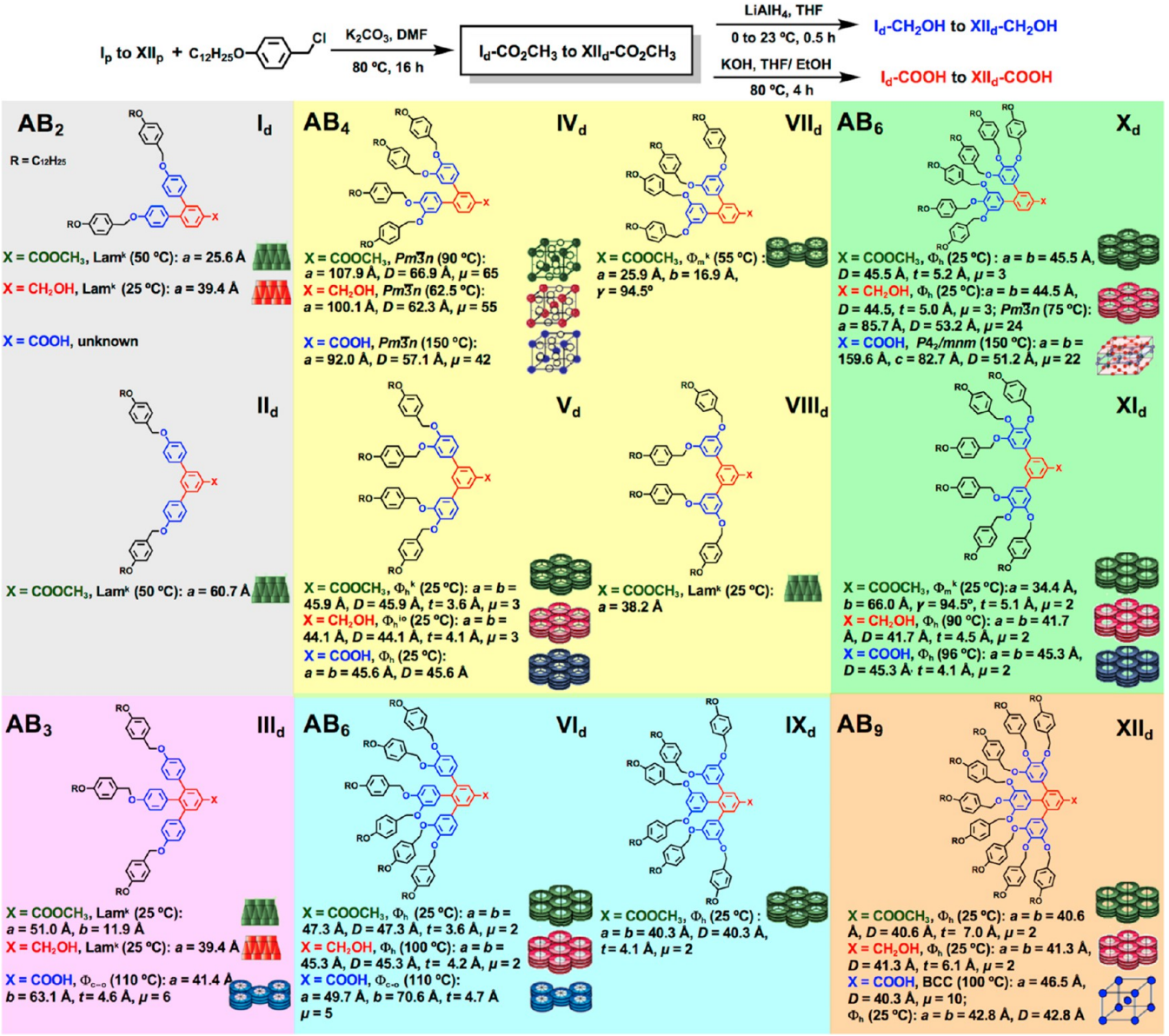

[a]Phase notations: Lam^k – crystalline lamellar; $Pm\bar{3}n$ – Frank-Kasper A15 phase; Φ_m^k – monoclinic columnar crystal; Φ_h – 2D columnar hexagonal array; Φ_{c-o} – 2D columnar centered orthorhombic array; Φ_h^k – 3D columnar hexagonal crystal. For sphere-containing phases, *D* denotes sphere diameter and μ denotes number of molecules with a supramolecular sphere. For columnar phases, *D* denotes column diameter and μ denotes number of molecules with a single column stratum. *D* and μ were calculated according to formulas detailed in the SI.

The building blocks from Tables 2, 3, S2, and S3 allowed the synthesis of nonsymmetric dendrons and supramolecular dendrimers in a single step by etherification of the corresponding phenolic esters with 4-(*n*-dodecyloxy)benzyl chloride under the same reaction conditions as discussed in the previous subchapter. Table 5 outlines the synthesis and the structural and retrostructural analysis of constitutional isomeric compounds with multiple substitution patterns: two AB_4 ($\mathbf{XIII_d}$, $\mathbf{XIV_d}$), three AB_5 ($\mathbf{XV_d}$, $\mathbf{XVIII_d}$, $\mathbf{XXI_d}$), two AB_6 ($\mathbf{XVII_d}$, $\mathbf{XX_d}$), three AB_7 ($\mathbf{XVI_d}$, $\mathbf{XIX_d}$, $\mathbf{XXII_d}$), and two AB_8 ($\mathbf{XXIII_d}$, $\mathbf{XXIV_d}$), while Table 6 summarizes two AB_3 ($\mathbf{XXV_d}$, $\mathbf{XXVI_d}$), two additional AB_4 ($\mathbf{XXVII_d}$, $\mathbf{XXVIII_d}$), and two additional AB_5 ($\mathbf{XXIX_d}$, $\mathbf{XXX_d}$). The results from Table 4 are supported by the data summarized in Tables 5 and 6. Unexpectedly, the two constitutionally isomeric AB_3 ($\mathbf{XXV_d}$, $\mathbf{XXVI_d}$) (Table 6) and the two AB_4 ($\mathbf{XIII_d}$, $\mathbf{XIV_d}$) (Table 5) self-assembling dendrons form lamellar assemblies representing 22% of all molecules from Tables 5 and 6. The two constitutional isomeric AB_3 ($\mathbf{XXV_d}$, $\mathbf{XXVI_d}$) (Table 6), the three AB_5 from Tables 5 and 6 ($\mathbf{XV_d}$ with X = $-CO_2CH_3$, $-CH_2OH$, $\mathbf{XVIII_d}$ with X = $-CO_2CH_3$, $-CH_2OH$, $-COOH$, and $\mathbf{XXIX_d}$ with X = $-CO_2CH_3$, $-CH_2OH$), one AB_6 ($\mathbf{XX_d}$ with X = $-CH_2OH$) (Table 5), the three AB_7 ($\mathbf{XVI_d}$ with X = $-CO_2CH_3$, CH_2OH, $\mathbf{XIX_d}$ with X = $-COOH$, and $\mathbf{XXII_d}$ with X = $-CO_2CH_3$, $-CH_2OH$) (Table 5), and the two AB_8 ($\mathbf{XXIII_d}$ with X = $-CO_2CH_3$, $-CH_2OH$ and $\mathbf{XXIV_d}$ with X = $-COOH$) (Table 5) form columnar assemblies, although, based on previous libraries[5,10,11,15,27,35] they were expected to

https://doi.org/10.1021/jacs.1c08502
J. Am. Chem. Soc. 2021, 143, 17724–17743

Table 5. Structural and Retrostructural Analysis of Supramolecular Dendrimers Self-Assembled from a Library of Nonsymmetric Constitutional Isomeric AB_4 to AB_8 Self-Assembling Dendrons

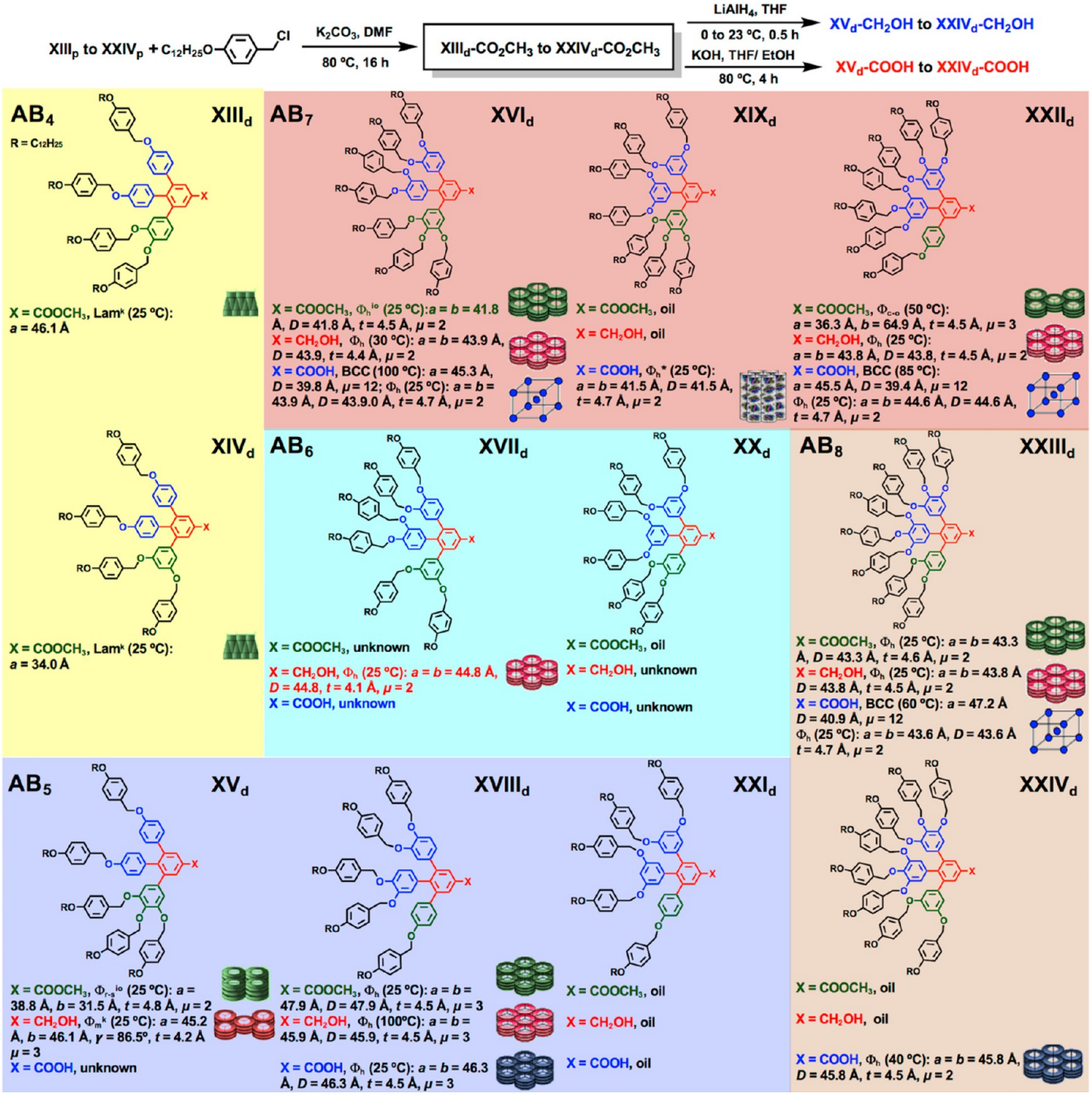

[a]Phase notations: Lam^k – crystalline lamellar; $Pm3n$ – Frank-Kasper A15 phase; BCC – body-centered cubic phase; Φ_m^k – monoclinic columnar crystal; Φ_h – 2D columnar hexagonal array; Φ_{r-s} – 2D columnar simple rectangular array; Φ_h^{io} – 2D columnar hexagonal array with intracolumnar order. For sphere-containing phases, D denotes sphere diameter and μ denotes number of molecules with a supramolecular sphere. For columnar phases, D denotes column diameter and μ denotes number of molecules with a single column stratum. D and μ were calculated according to formulas detailed in the SI.

generate spherical assemblies. They represent 61% of all molecules from Tables 5 and 6. This fraction could be even higher since **XX$_d$**, **XXI$_d$**, and **XXX$_d$** are oils at room temperature and may exhibit ordered phases that were not yet analyzed below room temperature, or even exhibit new unknown lattices whose structures were not yet elucidated. It is also interesting to observe that the AB_7 **XVI$_d$** with X = −COOH and **XXII$_d$** with X = −COOH, the AB_8 **XXIII$_d$** with X = −COOH (all from Table 5), and the AB_5 **XXIX$_d$** with X = −COOH (Table 6) form spherical assemblies that are all BCC. They represent 22% of all assemblies from Tables 5 and 6. No Frank−Kasper spherical phases were observed for any of the spherical nonsymmetric supramolecular dendrimers from Tables 5 and 6. A supramolecular columnar hexagonal lattice self-organized from supramolecular spheres was discovered for **XIX$_d$** with X = −COOH (Table 5). The discovery of columns

https://doi.org/10.1021/jacs.1c08502
J. Am. Chem. Soc. 2021, 143, 17724−17743

Table 6. Structural and Retrostructural Analysis of Supramolecular Dendrimers Self-Assembled from a Library of Nonsymmetric Constitutional Isomeric AB_3 to AB_5 Self-Assembling Dendrons

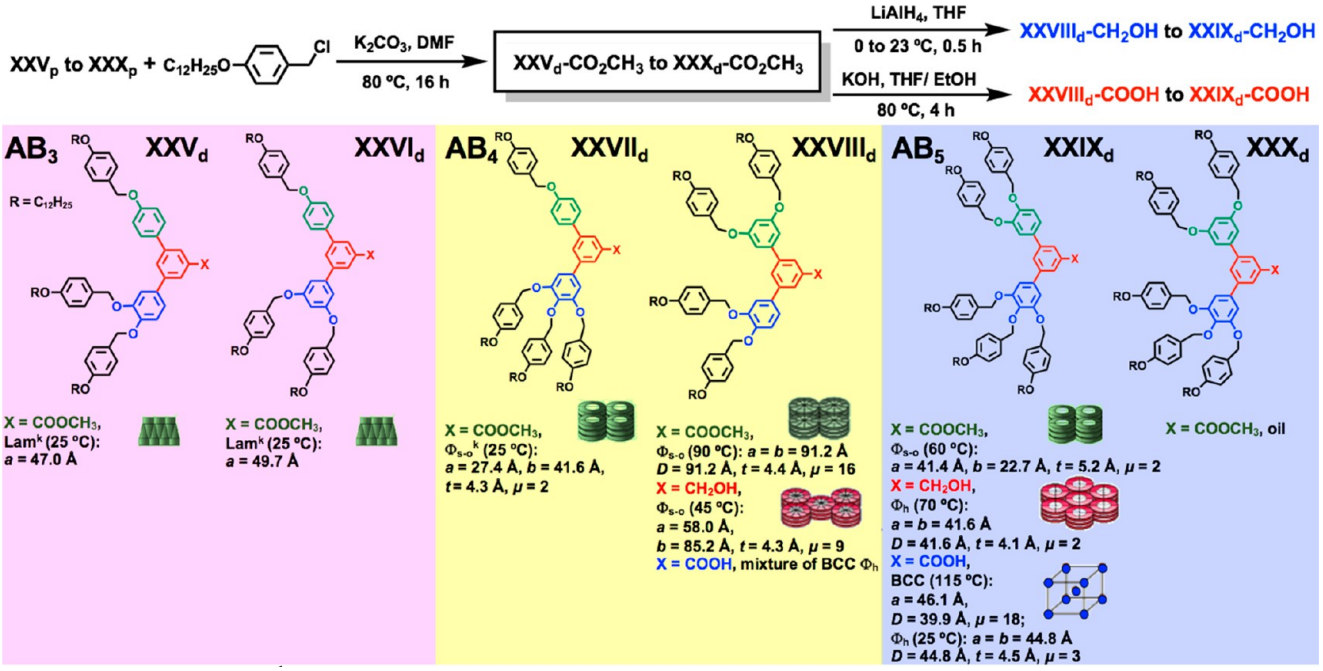

[a]Phase notations: Lam^k – crystalline lamellar; BCC – body-centered cubic phase; Φ_h – 2D columnar hexagonal array; Φ_{s-o} – 2D columnar simple orthorhombic array; Φ_{s-o}^k – columnar simple orthorhombic crystal. For sphere-containing phases, D denotes sphere diameter and μ denotes number of molecules with a supramolecular sphere. For columnar phases, D denotes column diameter and μ denotes number of molecules with a single column stratum. D and μ were calculated according to formulas detailed in the SI.

assembled from spheres was only recently reported by our laboratory[37] although undulated columns, which are expected to be precursors to spheres, were known before.[5]

Structural and Retrostructural Analysis of Selected Examples of TMV-like Helical Columns, Disorganized Nonhelical Columns, Frank–Kasper Phases, and Bilayer Arrays. Table 4 presents a collection of diverse but representative examples of self-organizations that are missing the sp^3–sp^3 bonds from their basic repeat unit. As noted above, there is a reduction in the number of supramolecular spheres forming Frank–Kasper phases from the previous libraries based on self-assembling benzyl ether and other ether dendrons.[17,18,27h] To rationalize this dramatic change in assembly behavior, it is instructive to first compare the helical columnar hexagonal crystal generated by $\mathbf{V_d}$ with X = $-CO_2CH_3$ (Figure 2a) with that of the corresponding benzyl ether (4-3,4-3,5)12G2-CO_2CH_3 (Figure 2f). This self-assembling benzyl ether dendron has been used in the synthesis of dendritic dipeptides[34b,38,39] that mimic the water channel Aquaporin.[40] The SAXS and WAXS of the oriented fibers obtained from both compounds are shown in Figure 2b, g. The SAXS patterns are similar but provide different diameters D = 56 Å for the benzyl ether and D = 46 Å for the helical column of $\mathbf{V_d}$. In contrast, the WAXS data are quite different, showing a highly ordered helical hexagonal crystal for $\mathbf{V_d}$ (Figure 2b) and a less ordered hexagonal crystal for the benzyl ether (Figure 2g).

The number of dendrons forming the cross section of the column is μ = 3 for $\mathbf{V_d}$ and 4 for the benzyl ether analogue. The spatial extent of a dendron in a columnar cross-section can be described by its solid angle,[41] whose projection is calculated for a planar disc as $360°/\mu$; therefore, the solid angle for $\mathbf{V_d}$ is 120° whereas for the benzyl ether counterpart (4-3,4-3,5)12G2-CO_2CH_3 it is 90°. The most remarkable difference between these two dendrons is that the solid angle of $\mathbf{V_d}$ is unchanged when the alkyl group on the periphery changes from *n*-dodecyl to *n*-hexyl (to be published) and, therefore, the number of dendrons in the cross section of the column remains constant. This is in stark contrast to the benzyl ether dendron, for which the solid angle and the number of dendrons forming the cross section of the column change continuously when the alkyl group of its periphery changes from *n*-hexyl to *n*-hexadecyl.[38a,d] This demonstrates that between *n*-dodecyl and *n*-hexyl $\mathbf{V_d}$ has a rigid solid angle of 120° while the benzyl ether dendron has an adaptable solid angle.[38a,d] As a consequence, $\mathbf{V_d}$ self-organizes into a triple 8_1 helix (or a 24_3 helix) consisting of 3 molecules that rotate by 15° in each column stratum (Figure 2c–e). The simulated X-ray diffractogram (Figure 2b, WAXS, right) for the model of $\mathbf{V_d}$ shown in Figure 2c–e shows good agreement with the experimental fiber XRD data (Figure 2b, WAXS, left). The weaker intensity of features on the L = 1 layer line in the experimental data compared to the simulated data suggests that column strata are not spaced with an exact 3.6 Å spacing, but instead that there is some minor degree of disorder with respect to stacking along the column axis. Molecular models were constructed, by the methodology elaborated in our laboratory and reported in previous publications,[27,35] by matching the experimental density with the density of the molecular model generated with the dimensions provided by X-ray analysis with Material Studio (version 5.0) software. The simulated X-ray from Figure 2b WAXS, right, was generated with Cerius 2 software.[27,35] These preliminary data provide the first example of a rigid solid angle that generates a mechanism

https://doi.org/10.1021/jacs.1c08502
J. Am. Chem. Soc. 2021, 143, 17724–17743

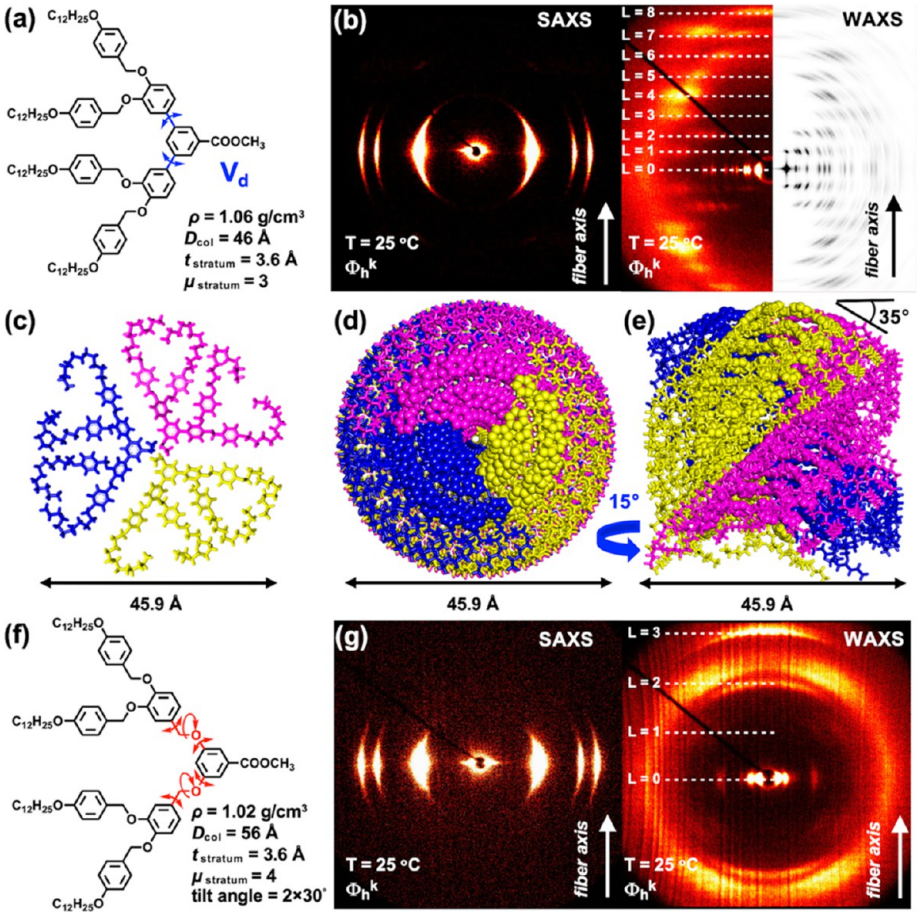

Figure 2. Helical supramolecular assembly of the 24_3 helix of $\mathbf{V_d}$. (a–e) Structural and retrostructural analysis of self-assembled $\mathbf{V_d}$. (f, g) Structural and retrostructural analysis of corresponding self-assembling dendron with benzyl ether connections, (4-3,4-3,5)12G2-CO_2CH_3. Colored arrows in (a) and (f) compare the number of rotational degrees of freedom in the sp^2–sp^2 (a) and benzyl ether (f) dendrons.

of helical self-organization and crystallization resembling TMV.[42] Both the helical self-organization of $\mathbf{V_d}$ and of the benzyl ether dendrons are sensitive to the functional group attached to their apex (Figure S15). A more detailed structural and mechanistic discussion of this self-organization process will be published elsewhere. Self-organization of all other columnar hexagonal arrays can be inspected by the fiber X-ray data from Figure S8. AB_6 $\mathbf{XI_d}$ with X = $-CO_2CH_3$ and $\mathbf{XVI_d}$ with X = $-CO_2CH_3$ show helical columnar structures with much lower degrees of crystallinity while all other columnar assemblies are highly disordered and nonhelical. The X-ray patterns of the A15 Frank–Kasper phase exhibited by $\mathbf{IV_d}$ with X = $-CO_2CH_3$, $-CH_2OH$, and $-COOH$ (Figure 3a–c) are shown in Figure 3f–h, and Figure 3k–m, and that of $\mathbf{XIX_d}$ with X = $-COOH$ (Figure 3d) is shown in Figure 3i,n, while that of the σ-phase of $\mathbf{X_d}$ with X = $-COOH$ (Figure 3e) is shown in Figure 3j,o. They agree with XRD patterns reported in the previous publications.[17a,c,35]

A very interesting feature is available in both the symmetric and nonsymmetric AB_2 $\mathbf{I_d}$, $\mathbf{II_d}$, AB_3 $\mathbf{III_d}$, AB_4 $\mathbf{VII_d}$, $\mathbf{XIII_d}$, $\mathbf{XIV_d}$, $\mathbf{XXVII_d}$, and $\mathbf{XXVIII_d}$ (Tables 4–6) compounds, which forms bilayer structures that are of interest as mimics of biological membranes and of their glycan, as models for endocytosis, as hybrid cells,[24] and for the delivery of mRNA.[25] Due to the nonsymmetric arrangement of their *n*-alkyl groups they are expected to provide highly soluble vesicles without needing to incorporate double bonds in their alkyl tails. An example of the bilayer structure of $\mathbf{VIII_d}$ to illustrate this concept is shown in Figure 4. The bilayer structures of all other compounds are shown in Figures S9–S14.

Columns from Spheres, Rarely Encountered BCC Phases, and Tetrahedral Bundles of Hexagonal Columns. Self-organization of supramolecular columns from supramolecular spheres is expected as a process during the transition from a columnar hexagonal array to a cubic lattice, and indeed these structures were observed recently for the first time during this process.[37a] Subsequently columns from spheres were discovered in the absence of this transition.[37a] $\mathbf{XIX_d}$ with X = $-COOH$ provides the second example of supramolecular columns assembled from supramolecular spheres (Table 5 and Figure 3d). The oriented fiber diffractogram of the columnar hexagonal array from Figure 3i is identical to the previous examples of columnar hexagonal arrays self-organized from spheres.[37] Before the discovery of the Frank–Kasper A15 phase in supramolecular dendrimers[11b,c,17a,b] followed by the σ-phase[17c] and LC quasicrystal,[18] it was expected that soft spheres self-organize predominantly in face-centered cubic (FCC) and body-centered cubic (BCC) lattices.[36a] In the meantime Frank–Kasper phases were discovered also in block copolymers,[19] surfactants,[20] giant molecules,[21] and DNA nanoparticles.[22]

The self-assembling dendrons reported in this publication provide a transition back to BCC phases since they self-organize predominantly in BCC rather than in Frank–Kasper

https://doi.org/10.1021/jacs.1c08502
J. Am. Chem. Soc. 2021, 143, 17724–17743

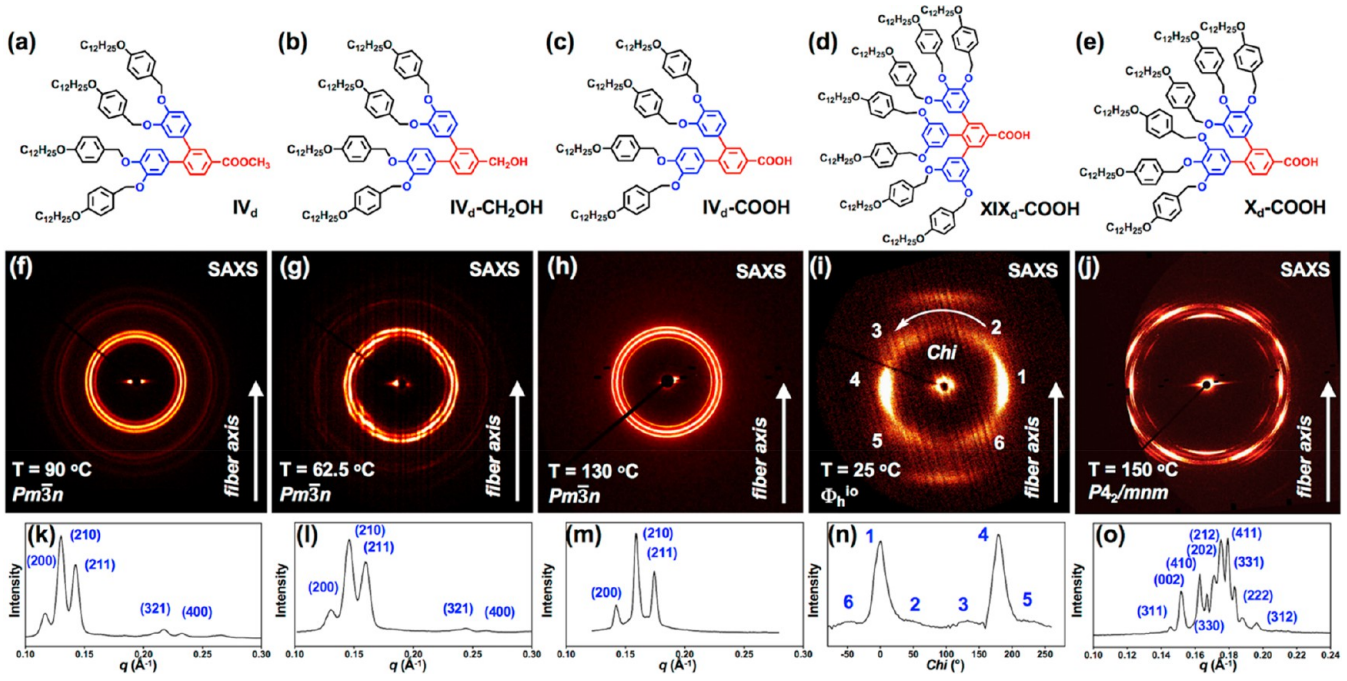

Figure 3. Structural analysis of supramolecular assemblies with selected phases. (a–e) Chemical structures of the self-assembling dendrons. XRD experiments data for A15 or *Pm*3*n* (f–h), column-from-sphere phases (i), and σ or $P4_2/mnm$ (j); (k–m, o) XRD diffractogram at given temperatures with assigned peaks. (n) Azimuthal plot of the columnar hexagonal with intracolumnar order ($\mathbf{\Phi_h}^{io}$) phase with corresponding features assigned.

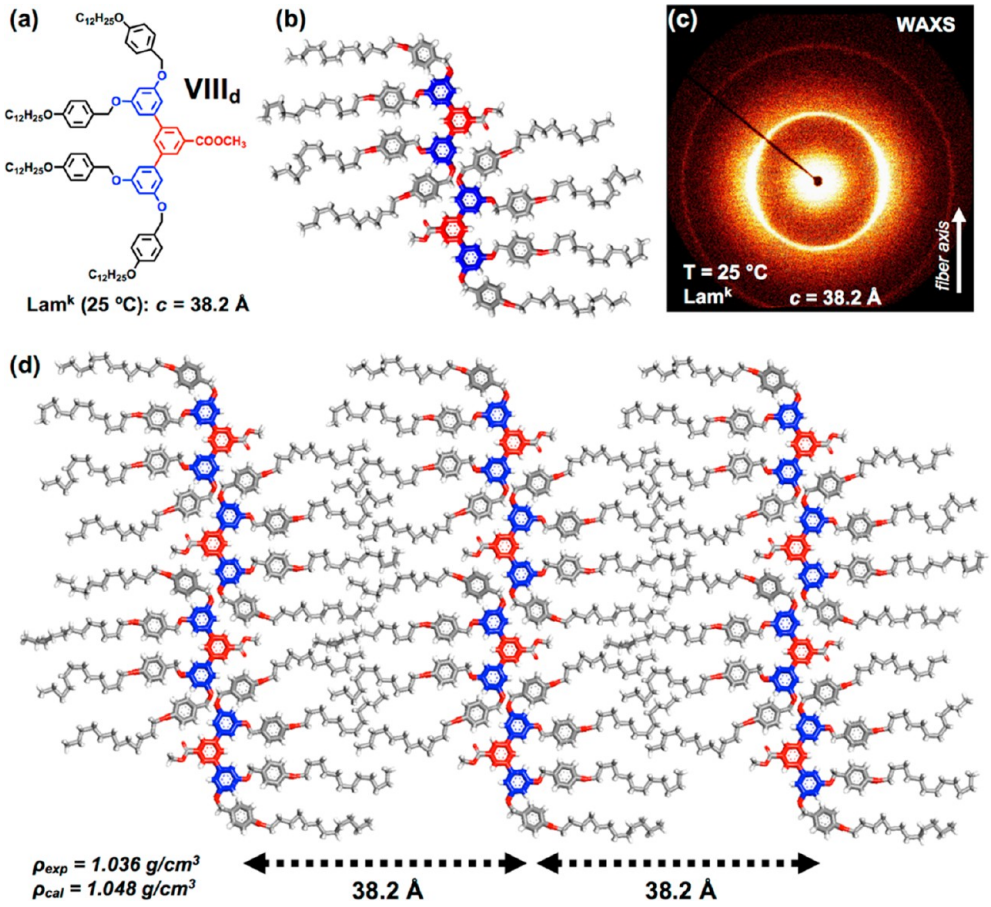

Figure 4. XRD patterns and molecular models of the crystalline lamellar (Lam^k) phase of **VIII$_d$**. (a) Chemical structure of **VIII$_d$**. (c) Experimental XRD pattern collected with a sample-to-detector distance of 0.07 m (WAXS). (b, d) Molecular models of the crystalline lamellar (Lam^k) phase.

https://doi.org/10.1021/jacs.1c08502
J. Am. Chem. Soc. 2021, 143, 17724–17743

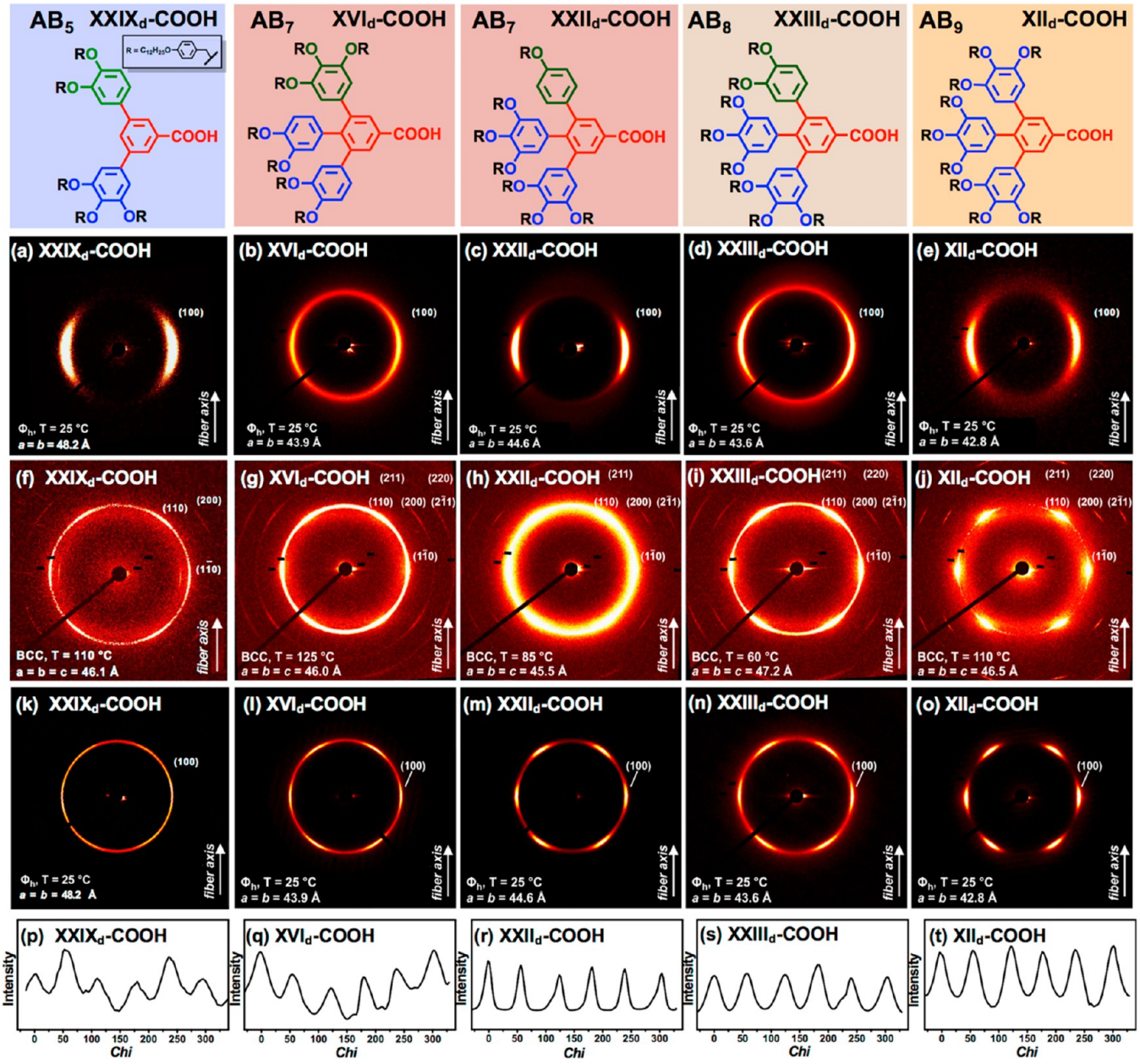

Figure 5. Small-angle (SAXS) oriented fiber XRD patterns recorded from highly ordered BCC assemblies self-organized from the AB_5 to AB_9 constitutional isomeric self-assembling dendrons. Chemical structures are shown on top of their XRD patterns.

phases. We expect that hybrid self-assembling dendrons based on benzyl ether and the currently reported building blocks will provide access to the prediction of all cubic and Frank−Kasper phases. Research toward this goal is in progress. Figure 5 summarizes the structures and the oriented fiber XRDs of five dendrons with COOH at their apex: AB_5 ($\mathbf{XXIX_d}$), AB_7 ($\mathbf{XVI_d}$ and $\mathbf{XXII_d}$), AB_8 ($\mathbf{XXIII_d}$), and AB_9 ($\mathbf{XII_d}$). These dendrons assemble columnar hexagonal arrays at 25 °C (Figure 5a−e) and transition to the BCC phase upon heating (Figure 5f−j). Upon cooling, these structures return to columnar hexagonal arrays (Figure 5k−o). However, in all cases, additional off-equatorial features corresponding to (100) are observed. The azimuthal distribution of these (100) features (Figure 5p−t) is consistent with previous reports[43] in which an epitaxial nucleation at the transition from BCC to the columnar hexagonal phase occurs along the four [111] directions of the BCC phase. This epitaxial phenomenon, which was termed supramolecular orientational memory (SOM) and is shown in detail for AB_9 $\mathbf{XII_d}$ in Figure 6, occurs because the spheres of the BCC lattice are in closest contact along their (111) directions (Figure 6e) that nucleate the formation of columns. This generates a tetrahedral arrangement of hexagonal columns upon cooling to the columnar hexagonal phase (Figure 6f).

This series of dendrons represents the largest group of structurally related molecules that exhibits an SOM effect. It is notable that, in all cases, the number of molecules in the supramolecular sphere of the BCC phase (μ in Tables 4−6) is an exact multiple of the number of molecules in the column stratum (μ in Tables 4−6): for AB_5 ($\mathbf{XXIX_d}$), μ = 18 (in sphere) and μ = 3 (in column stratum); for AB_9 ($\mathbf{XII_d}$), μ = 10 (in sphere) and μ = 2 (in columns stratum); and for the three AB_7 and AB_8 dendrons ($\mathbf{XVI_d}$, $\mathbf{XXII_d}$, and $\mathbf{XXIII_d}$), μ = 12 (in

https://doi.org/10.1021/jacs.1c08502
J. Am. Chem. Soc. 2021, 143, 17724−17743

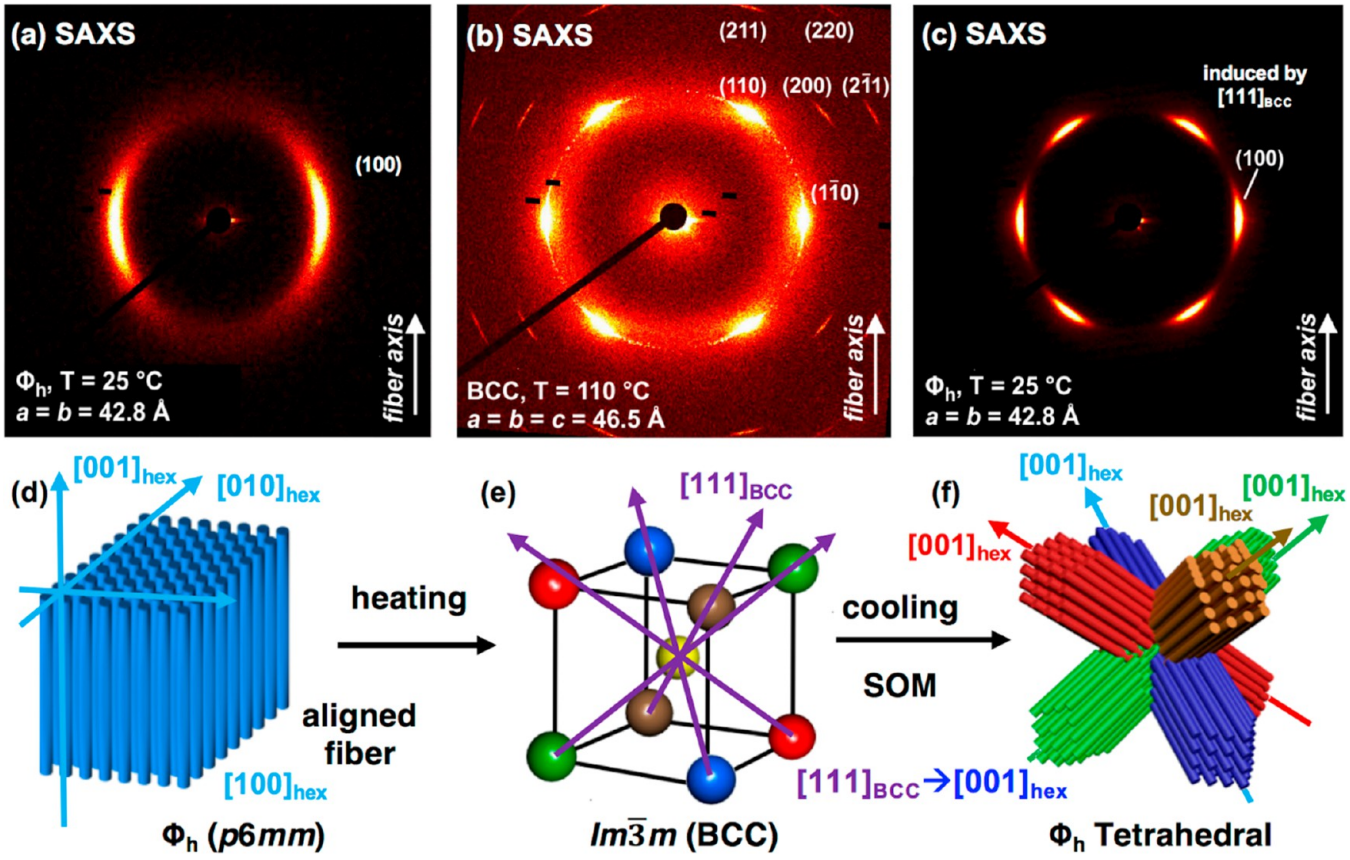

Figure 6. (a–c) XRD of an aligned fiber obtained by extrusion at 23 °C of $\mathbf{XII}_d$-COOH during first heating and cooling. Temperature and lattice parameters are indicated. (d–f) Schematic representation of the lattice transition between Φ_h and $Im\bar{3}m$ on first heating and cooling. SOM induced by $[111]_{BCC}$ to $[001]_{hex}$ results in a tetrahedral arrangement of columnar hexagonal domains.

sphere) and μ = 2 (in column stratum). This observation suggests that the transition between column and sphere can occur without disrupting the interaction between molecules within a single column stratum, which may arise due to hydrogen bonding between COOH apical groups. Harnessing intermolecular interactions within column strata may provide a route to generalize the SOM to additional structures. Supramolecular spheres self-assemble from conical or crown conformations of self-assembling dendrons.[37b,44]

Figure 7 demonstrates how the SOM effect provides the only methodology to discriminate between the two mechanisms of self-assembly of supramolecular spheres from $\mathbf{XII}_d$ with X = −COOH. Ten dendrons with either crown (Figure 7c) or conical (Figure 7d) conformations self-assemble into a supramolecular sphere with an identical diameter of 39.3 Å, and therefore these two possibilities cannot be discriminated by structural analysis alone. However, we recently demonstrated that only the crown conformation of the dendrons produces supramolecular spheres that undergo the SOM.[44e] Therefore, since the BCC lattice in which this sphere self-organizes undergoes a SOM process, the self-assembling dendron forming the sphere must adopt a crown conformation. More detailed analysis of all these BCC phases will be reported elsewhere. Although the chemical structure of the self-assembling AB_9 dendron $\mathbf{XII}_d$ seems to look like that of a dendrimer (Table 5, Figure 5),[1,10,35] its self-organization principles follow the mechanism of dendrons (Figure 7) rather than that of dendrons that reached the size and reactivity of the functional group at the focal point of dendrimers and therefore can be named either dendrons or dendrimers.[10,42g]

Cubic phases including BCC are the self-organizations of icosahedral viruses,[45a,c] dendronized metal salts, and salts solubilized by dendronized crown ethers display both Frank–Kasper and BCC phases.[45d,e] Therefore, the self-organizing principles of synthetic and biological matter seem to be similar if not identical.[42f,g] Polyphenylene dendrimers and hyperbranched polymers were previously prepared both by Pd-catalyzed cross-coupling in a convergent method[3b,46a–c] and by the Diels–Alder reaction.[46d–f] Nevertheless, they were not designed as self-assembling dendrons and were not employed in systematic studies to elucidate the mechanism of self-assembly.

CONCLUSIONS

Three libraries containing 30 symmetric and nonsymmetric constitutional isomeric, sequence-defined AB_2 to AB_9 phenolic esters were synthesized from natural phenols and phenolic acids by an accelerated modular-orthogonal Ni-catalyzed methodology with Ni-catalysts, all elaborated in our laboratory. A single etherification step with 4-(*n*-dodecyloxy)benzyl chloride rather than with minidendrons[35] transformed all phenolic esters into self-assembling dendrons, which represents unprecedented self-organizing principle for the field of self-organizing dendrons, dendrimers, and dendronized polymers. Additional unprecedented self-organizing principles refer to the diversity of self-assembling dendron architectures obtained after such a simple one-step etherification process of the

https://doi.org/10.1021/jacs.1c08502
J. Am. Chem. Soc. 2021, 143, 17724–17743

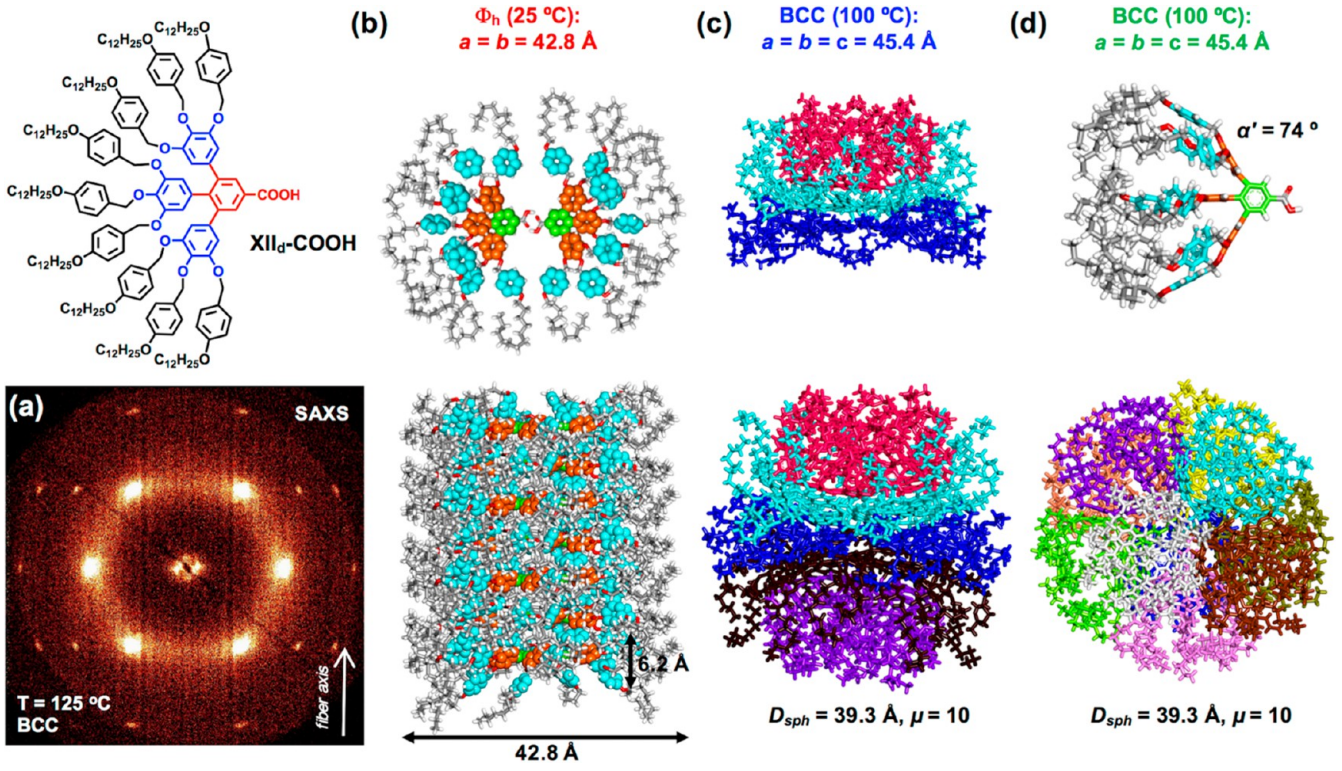

Figure 7. XRD patterns and molecular models of the body-centered cubic (BCC) phase of **XII$_d$**–COOH. (a) Experimental XRD pattern collected with a sample-to-detector distance of 0.54 m (SAXS). (b) Top view of the single layer (top) of the column forming the crystalline columnar hexagonal phases and the side view of the supramolecular column (bottom). (c) Upper half (top) and the whole structure (bottom) of the supramolecular sphere assembled from five crown dimeric conformers consisting of ten **XII$_d$**-COOH, side view. (d) Conical conformation of **XII$_d$**-COOH (top) and the corresponding supramolecular sphere (bottom) assembled from ten conical conformers of **XII$_d$**-COOH. Two mechanisms of self-organization, including crown conformation (c) and conical conformation (d), are presented.

starting phenolic acids building blocks. The first group of dendron architectures exhibiting these principles consists of lamellar structures of interest for amphiphilic Janus dendrimers, Janus glycodendrimers, and ionizable amine Janus dendrimers that function as biological membrane mimics and single component delivery systems for mRNA.[25] The second group of architectures provided the first helical columnar assemblies from rigid solid angle dendrons forming helical TMV-like assemblies. The third group provides disordered micellar-like nonhelical supramolecular columns *via* self-assembling dendrons with adaptable solid angles. Columns from spheres observed only infrequently before were also obtained. Five rarely encountered BCC phases displaying a supramolecular orientational memory (SOM) effect provided the fifth group of self-assembling dendrons. The sixth group self-organizes only two Frank–Kasper phases, A15 and σ. Cubic phases encountered in viruses, in dendronized metal salts, and in metal salts solubilized by dendronized crown ethers are complementary to those of the supramolecular dendrimers forming BCC assemblies reported here. Frank–Kasper phases were discovered in self-organizable dendrons, dendrimers, and dendronized polymers and subsequently in block copolymers, lipids, surfactants, giant molecules, and DNA nanoparticles. Finally, the ratio between sp^3–sp^3 and sp^2–sp^2 bonds in the self -assembling dendrons seems to determine the extent of entropy increase during the minimization of the supramolecular assemblies area,[36b] a self-organizing principle that we expect to be generalized for the engineering of soft and hard supramolecular spheres and of other objects in future experiments to be performed with the building blocks elaborated here. It could be that we were fortunate to start our investigations on self-organizable dendrons, dendrimers, and dendronized polymers with soft benzyl ether based assemblies and this facilitated the discovery of Frank–Kasper phases, and of quasicrystals.[11b,17a,b,d,18a,19f] Therefore, principles encountered in these new libraries of symmetric and nonsymmetric constitutional isomeric, sequence-defined dendrons, together with those of previous libraries, are expected to provide access to extended rational design principles for all cubic and Frank–Kasper phases as well as for helical and nonhelical columns and their bundles in synthetic and biological soft matter.[27h,47]

■ ASSOCIATED CONTENT

Supporting Information

The Supporting Information is available free of charge at https://pubs.acs.org/doi/10.1021/jacs.1c08502.

Experimental methods, synthesis, and characterization of building blocks, supramolecular dendrimers, DSC traces, X-ray analysis, tables with thermal transitions and X-ray data (PDF)

■ AUTHOR INFORMATION

Corresponding Author

Virgil Percec – *Roy & Diana Vagelos Laboratories, Department of Chemistry, University of Pennsylvania, Philadelphia, Pennsylvania 19104-6323, United States;* orcid.org/0000-0001-5926-0489; Email: percec@sas.upenn.edu

https://doi.org/10.1021/jacs.1c08502
J. Am. Chem. Soc. 2021, 143, 17724–17743

Authors

Shitao Wang − *Roy & Diana Vagelos Laboratories, Department of Chemistry, University of Pennsylvania, Philadelphia, Pennsylvania 19104-6323, United States;* Present Address: S.W.: State Key Laboratory of Organic−Inorganic Composites, Beijing University of Chemical Technology, Beijing 100029, China;; orcid.org/0000-0002-8601-3675

Ning Huang − *Roy & Diana Vagelos Laboratories, Department of Chemistry, University of Pennsylvania, Philadelphia, Pennsylvania 19104-6323, United States;* orcid.org/0000-0001-8874-3439

Benjamin E. Partridge − *Roy & Diana Vagelos Laboratories, Department of Chemistry, University of Pennsylvania, Philadelphia, Pennsylvania 19104-6323, United States;* Present Address: B.E.P.: Department of Chemistry and International Institute for Nanotechnology, Northwestern University, Evanston, Illinois 60208, United States;; orcid.org/0000-0003-2359-1280

Xuefeng Wang − *Roy & Diana Vagelos Laboratories, Department of Chemistry, University of Pennsylvania, Philadelphia, Pennsylvania 19104-6323, United States;* Present Address: X.W.: College of Chemistry and Pharmaceutical Sciences, Qingdao Agricultural University, Qingdao, Shandong 266109, China;

Dipankar Sahoo − *Roy & Diana Vagelos Laboratories, Department of Chemistry, University of Pennsylvania, Philadelphia, Pennsylvania 19104-6323, United States*

David J. Hoffman − *Roy & Diana Vagelos Laboratories, Department of Chemistry, University of Pennsylvania, Philadelphia, Pennsylvania 19104-6323, United States*

Jagadeesh Malineni − *Roy & Diana Vagelos Laboratories, Department of Chemistry, University of Pennsylvania, Philadelphia, Pennsylvania 19104-6323, United States*

Mihai Peterca − *Roy & Diana Vagelos Laboratories, Department of Chemistry, University of Pennsylvania, Philadelphia, Pennsylvania 19104-6323, United States;* orcid.org/0000-0002-7247-4008

Ryan L. Jezorek − *Roy & Diana Vagelos Laboratories, Department of Chemistry, University of Pennsylvania, Philadelphia, Pennsylvania 19104-6323, United States*

Na Zhang − *Roy & Diana Vagelos Laboratories, Department of Chemistry, University of Pennsylvania, Philadelphia, Pennsylvania 19104-6323, United States*

Hina Daud − *Roy & Diana Vagelos Laboratories, Department of Chemistry, University of Pennsylvania, Philadelphia, Pennsylvania 19104-6323, United States;* Present Address: H.D.: Lahore College for Women University, Jail Rd, Lahore, Punjab 54000, Pakistan;

Paul D. Sung − *Roy & Diana Vagelos Laboratories, Department of Chemistry, University of Pennsylvania, Philadelphia, Pennsylvania 19104-6323, United States*

Emily R. McClure − *Roy & Diana Vagelos Laboratories, Department of Chemistry, University of Pennsylvania, Philadelphia, Pennsylvania 19104-6323, United States;* Present Address: E.R.M.: Department of Chemistry, Northwestern University, Evanston, Illinois 60208.

Se Lin Song − *Roy & Diana Vagelos Laboratories, Department of Chemistry, University of Pennsylvania, Philadelphia, Pennsylvania 19104-6323, United States*

Complete contact information is available at: https://pubs.acs.org/10.1021/jacs.1c08502

Notes

The authors declare no competing financial interest.

■ ACKNOWLEDGMENTS

Financial support by the National Science Foundation (DMR-1807127, DMR-1720530, and DMR- 2104554), the Humboldt Foundation, and the P. Roy Vagelos Chair at Penn (all to V.P.) is gratefully acknowledged. S.W. thanks the Japan Society for the Promotion of Science (JSPS) for a postdoctoral fellowship. B.E.P. thanks the Howard Hughes Medical Institute for an International Graduate Student Research Fellowship. The authors thank Professors G. Ungar (University of Sheffield) and P. A. Heiney (University of Pennsylvania) for discussions of the X-ray analysis and Dr. Qi Xiao for editorial help.

■ REFERENCES

(1) (a) Fréchet, J. M. J., Tomalia, D. A., Eds. *Dendrimers and Other Dendritic Polymers*; Wiley: New York, 2001. (b) Tomalia, D. A., Christensen, J. B., Boas, U *Dendrimers, Dendrons, and Dendritic Polymers*; Cambridge University Press: Cambridge, 2012. (c) Newkome, G. R.; Moorefield, C. N.; Vögtle, F. *Dendrimers and Dendrons*; Wiley-VCH: Weinheim, 2001. (d) Vögtle, F.; Richardt, G.; Werner, N. *Dendrimer Chemistry*; Wiley-VCH: Weinheim, 2009. (e) Klajnert, B., Peng, L., Cena, V., Eds. *Dendrimers in Biomedical Applications*; RSC Publishing: Cambridge, 2013.

(2) (a) Buhleier, E.; Wehner, W.; Vögtle, F. Cascade"- and "Nonskid-Chain-like" Syntheses of Molecular Cavity Topologies. *Synthesis* **1978**, *1978*, 155−158. (b) Tomalia, D. A.; Baker, H.; Dewald, J.; Hall, M.; Kallos, G.; Martin, S.; Roeck, J.; Ryder, J.; Smith, P. A New Class of Polymers: Starburst-Dendritic Macromolecules. *Polym. J.* **1985**, *17*, 117−132. (c) Newkome, G. R.; Yao, Z.; Baker, G. R.; Gupta, V. K. Micelles. Part 1. Cascade molecules: a new approach to micelles. A [27]-arborol. *J. Org. Chem.* **1985**, *50*, 2003−2004.

(3) (a) Hawker, C. J.; Fréchet, J. M. J. Preparation of Polymers with Controlled Molecular Architecture. A New Convergent Approach to Dendritic Macromolecules. *J. Am. Chem. Soc.* **1990**, *112*, 7638−7647. (b) Miller, T. M.; Neenan, T. X. Convergent Synthesis of Monodisperse Dendrimers Based Upon 1,3,5-Trisubstituted benzenes. *Chem. Mater.* **1990**, *2*, 346−349. (c) Grayson, S. M.; Fréchet, J. M. J. Convergent Dendrons and Dendrimers: from Synthesis to Applications. *Chem. Rev.* **2001**, *101*, 3819−3868.

(4) Jishkariani, D.; MacDermaid, C. M.; Timsina, Y. N.; Grama, S.; Gillani, S. S.; Divar, M.; Yadavalli, S. S.; Moussodia, R.-O.; Leowanawat, P.; Camacho, A. M. B.; Walter, R.; Goulian, M.; Klein, M. L.; Percec, V. Self-Interrupted Synthesis of Sterically Hindered Aliphatic Polyamide Dendrimers. *Proc. Natl. Acad. Sci. U. S. A.* **2017**, *114*, E2275−E2284.

(5) (a) Rosen, B. M.; Peterca, M.; Huang, C.; Zeng, X.; Ungar, G.; Percec, V. Deconstruction as a Strategy for the Design of Libraries of Self-Assembling Dendrons. *Angew. Chem., Int. Ed.* **2010**, *49*, 7002−7005. (b) Percec, V.; Rudick, J. G.; Peterca, M.; Yurchenko, M. E.; Smidrkal, J.; Heiney, P. A. Supramolecular Structural Diversity among First-Generation Hybrid Dendrimers and Twin Dendrons. *Chem. - Eur. J.* **2008**, *14*, 3355−3362.

(6) Tomalia, D. A.; Naylor, A. M.; Goddard, W. A. Starburst Dendrimers: Molecular-Level Control of Size, Shape, Surface Chemistry, Topology, and Flexibility from Atoms to Macroscopic Matter. *Angew. Chem., Int. Ed. Engl.* **1990**, *29*, 138−175.

(7) Mourey, T. H.; Turner, S. R.; Rubinstein, M.; Frechet, J. M. J.; Hawker, C. J.; Wooley, K. L. Unique Behavior of Dendritic Macromolecules: Intrinsic Viscosity of Polyether Dendrimers. *Macromolecules* **1992**, *25*, 2401−2406.

(8) de Gennes, P. G.; Hervet, H. Statistics of ≪Starburst≫ Polymers. *J. Phys., Lett.* **1983**, *44*, 351−360.

(9) Schlüter, A. D.; Rabe, J. P. Dendronized Polymers: Synthesis, Characterization, Assembly at Interfaces, and Manipulation. *Angew. Chem., Int. Ed.* **2000**, *39*, 864−883.

(10) Percec, V.; Cho, W.-D.; Möller, M.; Prokhorova, S. A.; Ungar, G.; Yeardley, D. J. P. Design and Structural Analysis of the First Spherical Monodendron Self-Organizable in a Cubic Lattice. *J. Am. Chem. Soc.* **2000**, *122*, 4249−4250.
(11) (a) Percec, V.; Ahn, C.-H.; Barboiu, B. Self-Encapsulation, Acceleration and Control in the Radical Polymerization of Monodendritic Monomers via Self-Assembly. *J. Am. Chem. Soc.* **1997**, *119*, 12978−12979. (b) Percec, V.; Ahn, C.-H.; Ungar, G.; Yeardley, D. J. P.; Möller, M.; Sheiko, S. S. Controlling Polymer Shape through the Self-Assembly of Dendritic Side-Groups. *Nature* **1998**, *391*, 161−164. (c) Percec, V.; Ahn, C.-H.; Cho, W.-D.; Jamieson, A. M.; Kim, J.; Leman, T.; Schmidt, M.; Gerle, M.; Möller, M.; Prokhorova, S. A.; Sheiko, S. S.; Cheng, S. Z. D.; Zhang, A.; Ungar, G.; Yeardley, D. J. P. Visualizable Cylindrical Macromolecules with Controlled Stiffness from Backbones Containing Libraries of Self-Assembling Dendritic Side Groups. *J. Am. Chem. Soc.* **1998**, *120*, 8619−8631. (d) Holerca, M. N.; Peterca, M.; Partridge, B. E.; Xiao, Q.; Lligadas, G.; Monteiro, M. J.; Percec, V. Monodisperse Macromolecules by Self-Interrupted Living Polymerization. *J. Am. Chem. Soc.* **2020**, *142*, 15265−15270.
(12) (a) Percec, V.; Lee, M.; Heck, J.; Blackwell, H. E.; Ungar, G.; Alvarez-Castillo, A. Re-entrant Isotropic Phase in a Supramolecular Disc-Like Oligomer of 4-[3,4,5-Tris(*n*-dodecanyloxy)benzyloxy]-4'-[2-Vinyloxy)ethoixy]biphenyl. *J. Mater. Chem.* **1992**, *2*, 931−938. (b) Percec, V.; Heck, J.; Tomazos, D.; Falkenberg, F.; Blackwell, H.; Ungar, G. Self-Assembly of Taper-Shaped Monoesters of Oligo(Ethylene Oxide) with 3,4,5-Tris(p-Dodecyloxybenzyloxy)Benzoic Acid and of Their Polymethacrylates into Tubular Supramolecular Architectures Displaying a Columnar Mesophase. *J. Chem. Soc., Perkin Trans. 1* **1993**, 2799−2811. (c) Johansson, G.; Percec, V.; Ungar, G.; Abramic, D. Molecular Recognition Directed Self-Assembly of Tubular Liquid Crystalline and Crystalline Supramolecular Architectures from Taper Shaped (15-Crown-5)Methyl 3,4,5-Tris(*p*-alkyloxybenzyloxy)benzoatre and (15-Crown-5)Methyl 3,4,5-Tris(p-dodecyloxy)benzoare. *J. Chem. Soc., Perkin Trans. 1* **1994**, 447−459. (d) Percec, V.; Tomazos, D.; Heck, J.; Blackwell, H.; Ungar, G. Self-Assembly of Taper-Shaped Monoesters of Oligo(ethylene Oxide) with 3,4,5-Tris(N-dodecan-1-yloxy)benzoic Acid and Their Polymethacylates into Tubular Supramolecular Architectures Displaying a Columnar Hexagonal Mesophase. *J. Chem. Soc., Perkin Trans. 2* **1994**, 31−44. (e) Percec, V.; Schlueter, D.; Ronda, J. C.; Johansson, G.; Ungar, G.; Zhou, J. P. Tubular Architectures from Polymers with Tapered Side Groups. Assembly of Side Groups via a Rigid Helical Chain Conformation and Flexible Helical Chain Conformation Induced via the Assembly of Side Groups. *Macromolecules* **1996**, *29*, 1464−1472. (f) Percec, V.; Schlueter, D. Mechanistic Investigation of the Formation of Supramolecular Cylidrical Shaped Oligomers and Polymers by Living Ring Opening Metathesis Polymerization of a 7-Oxanorbornene Monomer Substituted with Two Tapered Monodendrons. *Macromolecules* **1997**, *30*, 5783−5790. (g) Percec, V.; Schlueter, D.; Ungar, G.; Cheng, S. Z. D.; Zhang, A. Hierarchical Control of Internal Superstructure, Diameter, and Stability of Supramolecular and Macromolecular Columns Generated from Tapered Monodendritic Building Blocks. *Macromolecules* **1998**, *31*, 1745−1762.
(13) (a) Percec, V. Bioinspired Supramolecular Liquid Crystals. *Philos. Trans. R. Soc., A* **2006**, *364*, 2709−2719. (b) Percec, V. Merging Macromolecular and Supramolecular Chemistry into Bioinspired Synthesis of Complex Systems. *Isr. J. Chem.* **2020**, *60*, 48−66.
(14) (a) Ihre, H.; Hult, A.; Söderlind, E. Synthesis, Characterization, and 1H NMR Self-Diffusion Studies of Dendritic Aliphatic Polyesters Based on 2,2-Bis(Hydroxymethyl)Propionic Acid and 1,1,1-Tris-(Hydroxyphenyl)Ethane. *J. Am. Chem. Soc.* **1996**, *118*, 6388−6395. (b) Ihre, H.; Hult, A.; Fréchet, J. M. J.; Gitsov, I. Double-Stage Convergent Approach for the Synthesis of Functionalized Dendritic Aliphatic Polyesters Based on 2,2-Bis(Hydroxymethyl)Propionic Acid. *Macromolecules* **1998**, *31*, 4061−4068. (c) Zubarev, E. R.; Pralle, M. U.; Sone, E. D.; Stupp, S. I. Self-Assembly of Dendron Rodcoil Molecules into Nanoribbons. *J. Am. Chem. Soc.* **2001**, *123*, 4105−4106. (d) Ihre, H.; Padilla De Jesús, O. L.; Fréchet, J. M. J. Fast and Convenient Divergent Synthesis of Aliphatic Ester Dendrimers by Anhydride Coupling. *J. Am. Chem. Soc.* **2001**, *123*, 5908−5917. (e) Kim, C.; Kim, K. T.; Chang, Y.; Song, H. H.; Cho, T.-Y.; Jeon, H.-J. Supramolecular Assembly of Amide Dendrons. *J. Am. Chem. Soc.* **2001**, *123*, 5586−5587. (f) Kato, T. Self-Assembly of Phase-Segregated Liquid Crystal Structures. *Science* **2002**, *295*, 2414−2418. (g) Liang, C. O.; Helms, B.; Hawker, C. J.; Fréchet, J. M. J. Dendronized Cyclocopolymers with a Radial Gradient of Polarity and Their Use to Catalyze a Difficult Esterification. *Chem. Commun.* **2003**, *20*, 2524−2525. (h) Amir, R. J.; Pessah, N.; Shamis, M.; Shabat, D. Self-Immolative Dendrimers. *Angew. Chem., Int. Ed.* **2003**, *42*, 4494−4499. (i) Messmore, B. W.; Hulvat, J. F.; Sone, E. D.; Stupp, S. I. Synthesis, Self-Assembly, and Characterization of Supramolecular Polymers from Electroactive Dendron Rodcoil Molecules. *J. Am. Chem. Soc.* **2004**, *126*, 14452−14458. (j) Yoo, Y.-S.; Choi, J.-H.; Song, J. H.; Oh, N.-K.; Zin, W.-C.; Park, S.; Chang, T.; Lee, M. *J. Am. Chem. Soc.* **2004**, *126*, 6294−6300. (k) Cho, B.-K.; Jain, A.; Gruner, S. M.; Wiesner, U. Mesophase Structure-Mechanical and Ionic Transport Correlations in Extended Amphiphilic Dendrons. *Science* **2004**, *305*, 1598−1601. (l) Donnio, B.; Guillon, D. Liquid Crystalline Dendrimers and Polypedes. In *Supramolecular Polymers Polymeric Betains Oligomers*; Donnio, B., Guillon, D., Harada, A., Hashidzume, A., Jaeger, W., Janowski, B., Kudaibergenov, S., Laschewsky, A., Njuguna, J., Pielichowski, J., Pielichowski, K., Takashima, Y., Eds.; Springer-Verlag Berlin: Berlin, 2006; Vol. *201*, pp 45−155. (m) Bury, I.; Heinrich, B.; Bourgogne, C.; Guillon, D.; Donnio, B. Supramolecular Self-Organization of "Janus-like" Diblock Codendrimers: Synthesis, Thermal Behavior, and Phase Structure Modeling. *Chem. - Eur. J.* **2006**, *12*, 8396−8413. (n) Canilho, N.; Kasëmi, E.; Mezzenga, R.; Schlüter, A. D. Liquid-Crystalline Polymers from Cationic Dendronized Polymer-Anionic Lipid Complexes. *J. Am. Chem. Soc.* **2006**, *128*, 13998−13999. (o) Zhang, X.; Chen, Z.; Würthner, F. Morphology Control of Fluorescent Nanoaggregates by Co-Self-Assembly of Wedge- and Dumbbell-Shaped Amphiphilic Perylene Bisimides. *J. Am. Chem. Soc.* **2007**, *129*, 4886−4887. (p) Park, C.; Lim, J.; Yun, M.; Kim, C. Photoinduced Release of Guest Molecules by Supramolecular Transformation of Self-Assembled Aggregates Derived from Dendrons. *Angew. Chem., Int. Ed.* **2008**, *47*, 2959−2963. (q) Li, W.; Zhang, A.; Feldman, K.; Walde, P.; Schlüter, A. D. Thermoresponsive Dendronized Polymers. *Macromolecules* **2008**, *41*, 3659−3667. (r) Ornelas, C.; Broichhagen, J.; Weck, M. Strain-Promoted Alkyne Azide Cycloaddition for the Functionalization of Poly(Amide)-Based Dendrons and Dendrimers. *J. Am. Chem. Soc.* **2010**, *132*, 3923−3931. (s) Huang, Z.; Kang, S.-K.; Banno, M.; Yamaguchi, T.; Lee, D.; Seok, C.; Yashima, E.; Lee, M. Pulsating Tubules from Noncovalent Macrocycles. *Science* **2012**, *337*, 1521−1526. (t) Miyajima, D.; Araoka, F.; Takezoe, H.; Kim, J.; Kato, K.; Takata, M.; Aida, T. Ferroelectric Columnar Liquid Crystal Featuring Confined Polar Groups Within Core-Shell Architecture. *Science* **2012**, *336*, 209−213. (u) Jishkariani, D.; Diroll, B. T.; Cargnello, M.; Klein, D. R.; Hough, L. A.; Murray, C. B.; Donnio, B. Dendron-Mediated Engineering of Interparticle Separation and Self-Assembly in Dendronized Gold Nanoparticles Superlattices. *J. Am. Chem. Soc.* **2015**, *137*, 10728−10734. (v) Nummelin, S.; Liljestrom, V.; Saarikoski, E.; Ropponen, J.; Nykanen, A.; Linko, V.; Seppala, J.; Hirvonen, J.; Ikkala, O.; Bimbo, L. M.; Kostiainen, M. A. Self-Assembly of Amphiphilic Janus Dendrimers into Mechanically Robust Supramolecular Hydrogels for Sustained Drug Release. *Chem. - Eur. J.* **2015**, *21*, 14433−14439. (w) Guerra, S.; Iehl, J.; Holler, M.; Peterca, M.; Wilson, D. A.; Partridge, B. E.; Zhang, S.; Deschenaux, R.; Nierengarten, J.-F.; Percec, V. Self-Organisation of Dodeca-Dendronized Fullerene into Supramolecular Discs and Helical Columns Containing a Nanowire-like Core. *Chem. Sci.* **2015**, *6*, 3393−3401. (x) Wei, T.; Chen, C.; Liu, J.; Liu, C.; Posocco, P.; Liu, X.; Cheng, Q.; Huo, S.; Liang, Z.; Fermeglia, M.; Pricl, S.; Liang, X.-J.; Rocchi, P.; Peng, L. Anticancer Drug Nanomicelles Formed by Self-Assembling Amphiphilic Dendrimer to Combat Cancer Drug

https://doi.org/10.1021/jacs.1c08502
J. Am. Chem. Soc. 2021, 143, 17724−17743

Resistance. *Proc. Natl. Acad. Sci. U. S. A.* **2015**, *112*, 2978−2983. (y) Matsubara, M.; Stevenson, W.; Yabuki, J.; Zeng, X.; Dong, H.; Kojima, K.; Chichibu, S. F.; Tamada, K.; Muramatsu, A.; Ungar, G.; Kanie, K. A Low-Symmetry Cubic Mesophase of Dendronized CdS Nanoparticles and Their Structure-Dependent Photoluminescence. *Chem.* **2017**, *2*, 860−876. (z) Su, Z.; Zhang, R.; Yan, X.-Y.; Guo, Q.-Y.; Huang, J.; Shan, W.; Liu, Y.; Liu, T.; Huang, M.; Cheng, S. Z. D. The Role of Architectural Engineering in Macromolecular Self-Assemblies via Non-Covalent Interactions: A Molecular LEGO Approach. *Prog. Polym. Sci.* **2020**, *103*, 101230.

(15) (a) Percec, V.; Schlueter, D.; Kwon, Y. K.; Blackwell, J.; Muller, M.; Slangen, P. J. Dramatic Stabilization of Hexagonal Columnar Mesiophase Generated from Supramolecular and Macromolecular Columns by the Semifluorination of the Alkyl Groups of their Tapered Building Blocks. *Macromolecules* **1995**, *28*, 8807−8815. (b) Johansson, G.; Percec, V.; Ungar, G.; Zhou, J. P. Fluorophobic Effect in the Self-Assembly of Polymers and Model Compounds Containing Tapered Groups into Supramolecular Columns. *Macromolecules* **1996**, *29*, 646−660. (c) Percec, V.; Johansson, G.; Ungar, G.; Zhou, J. Fluorophobic Effect Induces the Self-Assembly of Semifluorinated Tapered Monodendrons Containing Crown Ethers into Supramole cular Columnar Dendrimers Which Exhibit a Homeotropic Hexagonal Columnar Liquid Crystalline Phase. *J. Am. Chem. Soc.* **1996**, *118*, 9855−9866. (d) Percec, V.; Bera, T. K. Cell Membrane as a Model for the Design of Semifluorinated Ion-Selective Nanostructured Supramolecular Systems. *Tetrahedron* **2002**, *58*, 4031−4040. (e) Percec, V.; Glodde, M.; Bera, T. K.; Miura, Y.; Shiyanovskaya, I.; Singer, K. D.; Balagurusamy, V. S. K.; Heiney, P. A.; Schnell, I.; Rapp, A.; Spiess, H.-W.; Hudson, S. D.; Duan, H. Self-Organization of Supramolecular Helical Dendrimers into Complex Electronic Materials. *Nature* **2002**, *419*, 384−387. (f) Percec, V.; Glodde, M.; Johansson, G.; Balagurusamy, V. S. K.; Heiney, P. A. Transformation of a Spherical Supramolecular Dendrimer into a Pyramidal Columnar Supramolecular Dendrimer Mediated by the Fluorophobic Effect. *Angew. Chem., Int. Ed.* **2003**, *42*, 4338−4342. (g) Percec, V.; Glodde, M.; Peterca, M.; Rapp, A.; Schnell, I.; Spiess, H. W.; Bera, T. K.; Miura, Y.; Balagurusamy, V. S. K.; Aqad, E.; Heiney, P. A. Self-Assembly of Semifluorinated Dendronas Attached to Electron-Donoir Groupd Mediates their pi-Stacking via a Helical Pyramidal Column. *Chem. - Eur. J.* **2006**, *12*, 6298−6314. (h) Percec, V.; Aqad, E.; Peterca, M.; Imam, M. R.; Glodde, M.; Bera, T. K.; Miura, Y.; Balagurusamy, V. S. K.; Ewbank, P. C.; Wurthner, F. W.; Heiney, P. A. Self-Assembly of Semifluorinated Minidendrons Attached to Electron-Acceptor Groups into Pyramidal Columns. *Chem. - Eur. J.* **2007**, *13*, 3330−3345. (i) Wu, Y.-C.; Leowanawat, P.; Sun, H.-J.; Partridge, B. E.; Peterca, M.; Graf, R.; Spiess, H. W.; Zeng, X. B.; Ungar, G.; Hsu, C.-S.; Heiney, P. A.; Percec, V. Complex Columnar Hexagonal Polymorphism in Supramolecular Assemblies of a Semifluorinated Electron-Accepting Naphthalene Bisimide. *J. Am. Chem. Soc.* **2015**, *137*, 807−819. (j) Ho, M. S.; Partridge, B. E.; Sun, H.-J.; Sahoo, D.; Leowanawat, P.; Peterca, M.; Graf, R.; Spiess, H. W.; Zeng, X. B.; Ungar, G.; Heiney, P. A.; Hsu, C.-S.; Percec, V. Screening Libraries of Semifluorinated Arylene Bisimides to Discover and Predict Thermodynamically Controlled Helical Crystallization. *ACS Comb. Sci.* **2016**, *18*, 723−739.

(16) (a) Percec, V.; Heck, J.; Lee, M.; Ungar, G.; Alvarez-Castillo, A. Poly{2-Vinyoxyethyl 3,4,5-Tris[4-(*n*-Dodecanyloxy)benzyloxy]-Benzoate}: A Self-Assembled Supramolecular Polymer Similat to Tobacco Mosaic Virus. *J. Mater. Chem.* **1992**, *2*, 1033−1039. (b) Kwon, Y. K.; Chvalun, S.; Schneider, A.-I.; Blackwell, J.; Percec, V.; Heck, J. A. Supramolecular Tubular Structures of a Polymethacrylate with Tapered Side Groups in Aligned Hexagonal Phases. *Macromolecules* **1994**, *27*, 6129−6132. (c) Kwon, Y. K.; Chvalun, S. N.; Blackwell, J.; Percec, V.; Heck, J. A. Effect of Temperature on the Supramolecular Tubular Structure in Oriented Fibers of a Polymethacrylate with Tapered Side Groups. *Macromolecules* **1995**, *28*, 1552−1558. (d) Percec, V.; Johansson, G.; Tomazos, D. Towards Tobacco Mosaic Virus-Like Self-Assembled Supramolecular Architectures. *Macromol. Symp.* **1994**, *77*, 237−267. (e) Percec, V.; Ungar, G.; Peterca, M. Self-Assembly in Action. *Science* **2006**, *313*, 55−56. (f) Andreopoulou, K. A.; Peterca, M.; Wilson, D. A.; Partridge, B. E.; Heiney, P. A.; Percec, V. Demonstrating the 8_1-Helicity and Nanomechanical Function of Self-Organizable Dendronized Polymethacylates and Polyacrylates. *Macromolecules* **2017**, *50*, 5271−5284. (g) Percec, V.; Rudick, J. G.; Peterca, M.; Obata, M.; Mitchell, C. M.; Cho, W. E. D.; Balagurusamy, V. S. K.; Heiney, P. A. Thermoreversible Cis-cisoidal to Cis-transoidal Isomerizatioon of Helical Dendronized Polyphenylacetylenes. *J. Am. Chem. Soc.* **2005**, *127*, 15257−15264. (h) Rudick, J. G.; Percec, V. Induced Helical Backbone Conformations of Self-Organizable Dendronized Polymers. *Acc. Chem. Res.* **2008**, *41*, 1641−1652. (i) Roche, C.; Sun, H. J.; Leowanawat, P.; Araoka, F.; Partridge, B. E.; Peterca, M.; Wilson, D. A.; Prendergast, M. E.; Heiney, P. A.; Graf, R.; Spiess, W. H.; Zeng, X. B.; Ungar, G.; Percec, V. Homochiral Columns by Chiral Self-Sorting During Supramolecxular Helical Organization o Hat-Shaped Molecules. *J. Am. Chem. Soc.* **2014**, *136*, 7169−7185. (j) Roche, C.; Sun, H. J.; Prendergast, M. E.; Leowanawat, P.; Partridge, B. E.; Heiney, P. A.; Araoka, F.; Graf, R.; Spiess, W. H.; Zeng, X. B.; Ungar, G.; Percec, V. A Supramolecular Helix that Dispegards Chirality. *Nat. Chem.* **2016**, *8*, 80−89. (k) Partridge, B. E.; Wang, L.; Sahoo, D.; Olsen, J. T.; Leowanawat, P.; Roche, C.; Ferreira, H.; Reilly, K. J.; Zeng, X. B.; Ungar, G.; Heiney, P. A.; Graf, R.; Spiess, W. H.; Percec, V. J. *J. Am. Chem. Soc.* **2019**, *141*, 15761−15766. (l) Wang, L.; Partridge, B. E.; Huang, N.; Olsen, J. T.; Sahoo, D.; Zeng, X. B.; Ungar, G.; Graf, R.; Spiess, W. H.; Percec, V. J. *J. Am. Chem. Soc.* **2020**, *142*, 9525−9536.

(17) (a) Balagurusamy, V. S. K.; Ungar, G.; Percec, V.; Johansson, G. Rational Design of the First Spherical Supramolecular Dendrimers Self-Organized in a Novel Thermotropic Cubic Liquid-Crystalline Phase and the Determination of Their Shape by X-Ray Analysis. *J. Am. Chem. Soc.* **1997**, *119*, 1539−1555. (b) Hudson, S. D.; Jung, H.-T.; Percec, V.; Cho, W.-D.; Johansson, G.; Ungar, G.; Balagurusamy, V. S. K. Direct Visualization of Individual Cylindrical and Spherical Supramolecular Dendrimers. *Science* **1997**, *278*, 449−452. (c) Dukeson, D. R.; Balagurusamy, V. S. K.; Percec, V.; Johansson, G. A.; Glodde, M. Application of Isomorphous Replacement in the Structure Determination of a Cubic Liquid Crystal Phase and Location of Counterions. *J. Am. Chem. Soc.* **2003**, *125*, 15974−15980. (d) Ungar, G.; Liu, Y.; Zeng, X.; Percec, V.; Cho, W.-D. Giant Supramolecular Liquid Crystal Lattice. *Science* **2003**, *299*, 1208−1211.

(18) (a) Zeng, X.; Ungar, G.; Liu, Y.; Percec, V.; Dulcey, A. E.; Hobbs, J. K. Supramolecular Dendritic Liquid Quasicrystals. *Nature* **2004**, *428*, 157−160. (b) Ungar, G.; Percec, V.; Zeng, X.; Leowanawat, P. Liquid Quasicrystals. *Isr. J. Chem.* **2011**, *51*, 1206−1215.

(19) (a) Lee, S.; Bluemle, M. J.; Bates, F. S. Discovery of a Frank-Kasper σ-Phase in Sphere-Forming Block Copolymer Melts. *Science* **2010**, *330*, 349−353. (b) Fischer, S.; Exner, A.; Zielske, K.; Perlich, J.; Deloudi, S.; Steurer, W.; Lindner, P.; Förster, S. Colloidal Quasicrystals with 12-Fold and 18-Fold Diffraction Symmetry. *Proc. Natl. Acad. Sci. U. S. A.* **2011**, *108*, 1810−1814. (c) Zhang, J.; Bates, F. S. Dodecagonal Quasicrystalline Morphology in a Poly(Styrene-b-Isoprene-b-Styrene-b-Ethylene Oxide) Tetrablock Terpolymer. *J. Am. Chem. Soc.* **2012**, *134*, 7636−7639. (d) Gillard, T. M.; Lee, S.; Bates, F. S. Dodecagonal Quasicrystalline Order in a Diblock Copolymer Melt. *Proc. Natl. Acad. Sci. U. S. A.* **2016**, *113*, 5167−5172. (e) Kim, K.; Schulze, M. W.; Arora, A.; Lewis, R. M., III; Hillmyer, M. A.; Dorfman, K. D.; Bates, F. S. Thermal Processing of Diblock Copolymer Melts Mimics Metallurgy. *Science* **2017**, *356*, 520−523. (f) Peterca, M.; Percec, V. Recasting Metal Alloy Phases with Block Copolymers. *Science* **2010**, *330*, 333−334.

(20) (a) Perroni, D. V.; Mahanthappa, M. K. Inverse *Pm*3*n* Cubic Micellar Lyotropic Phases from Zwitterionic Triazolium Gemini Surfactants. *Soft Matter* **2013**, *9*, 7919−7922. (b) Kim, S. A.; Jeong, K.-J.; Yethiraj, A.; Mahanthappa, M. K. Low-Symmetry Sphere Packings of Simple Surfactant Micelles Induced by Ionic Sphericity. *Proc. Natl. Acad. Sci. U. S. A.* **2017**, *114*, 4072−4077. (c) Baez-Cotto, C. M.; Mahanthappa, M. K. Micellar Mimicry of Intermetallic C14 and C15 Laves Phases by Aqueous Lyotropic Self-Assembly. *ACS*

https://doi.org/10.1021/jacs.1c08502
J. Am. Chem. Soc. 2021, 143, 17724−17743

Nano **2018**, *12*, 3226−3234. (d) Jayaraman, A.; Zhang, D. Y.; Dewing, B. L.; Mahanthappa, M. K. Path-Dependent Preparation of Complex Micelle Packings of a Hydrated Diblock Oligomer. *ACS Cent. Sci.* **2019**, *5*, 619−628. (e) Jayaraman, A.; Baez-Cotto, C. M.; Mann, T. J.; Mahanthappa, M. K. Dodecagonal Quasicrystals of Oil-Swollen Ionic Surfactant Micelles. *Proc. Natl. Acad. Sci. U. S. A.* **2021**, *118*, No. e2101598118.

(21) (a) Huang, M.; Hsu, C.-H.; Wang, J.; Mei, S.; Dong, X.; Li, Y.; Li, M.; Liu, H.; Zhang, W.; Aida, T.; Zhang, W.-B.; Yue, K.; Cheng, S. Z. D. Selective Assemblies of Giant Tetrahedra *via* Precisely Controlled Positional Interactions. *Science* **2015**, *348*, 424−428. (b) Yue, K.; Huang, M.; Marson, R. L.; He, J.; Huang, J.; Zhou, Z.; Wang, J.; Liu, C.; Yan, X.; Wu, K.; Guo, Z.; Liu, H.; Zhang, W.; Ni, P.; Wesdemiotis, C.; Zhang, W.-B.; Glotzer, S. C.; Cheng, S. Z. D. Geometry Induced Sequence of Nanoscale Frank-Kasper and Quasicrystal Mesophases in Giant Surfactants. *Proc. Natl. Acad. Sci. U. S. A.* **2016**, *113*, 14195−14200. (c) Feng, X.; Zhang, R.; Li, Y.; Hong, Y. L.; Guo, D.; Lang, K.; Wu, K. Y.; Huang, M.; Mao, J.; Wesdemiotis, C.; Nishiyama, Y.; Zhang, W.; Zhang, W.; Miysohi, T.; Li, T.; Cheng, S. Z. D. Hierarchical Self-Organization of AB_n Dendron-like Molecules into a Supramolecular Lattice Sequence. *ACS Cent. Sci.* **2017**, *3*, 860−867. (d) Su, Z.; Hsu, C.; Gong, Z.; Feng, X.; Huang, J.; Zhang, R.; Wang, Y.; Mao, J.; Wesdemiotis, C.; Li, T.; Seifert, S.; Zhang, W.; Aida, W.; Huang, M.; Cheng, S. Z. D. Identification of a Frank-Kasper Z from Shape Amphiphile Self-Assembly. *Nat. Chem.* **2019**, *11*, 899−905. (e) Liu, Y.; Liu, T.; Yan, X.; Guo, Q.-Y.; Wang, J.; Zhang, R.; Zhang, S.; Su, Z.; Huang, J.; Liu, G.-X.; Zhang, W.; Zhang, W.; Aida, T.; Yue, K.; Huang, M.; Cheng, S. Z. D. Mesoatom Alloys via Self-Sorting Approach of Giant Molecules Blends. *Giant* **2020**, *4*, 100031.

(22) Girard, M.; Wang, S.; Du, J. S.; Das, A.; Huang, Z.; Dravid, V. P.; Lee, B.; Mirkin, C. A.; Olvera de la Cruz, M. Particle Analogs of Electrons in Colloidal Crystals. *Science* **2019**, *364*, 1174−1178.

(23) (a) Lachmayr, K. K.; Wentz, C. M.; Sita, L. R. An Exceptionally Stable and Scalable Sugar-Polyolefin Frank-Kasper A15 Phase. *Angew. Chem., Int. Ed.* **2020**, *59*, 1521−1526. (b) Lachmayr, K. K.; Sita, L. R. Small-Molecule Modulation of Soft-Matter Frank-Kasper Phases: A Method for Adding Function to Form. *Angew. Chem., Int. Ed.* **2020**, *59*, 3563−3567.

(24) (a) Percec, V.; Wilson, D. A.; Leowanawat, P.; Wilson, C. J.; Hughes, A. D.; Kaucher, M. S.; Hammer, D. A.; Levine, D. H.; Kim, A. J.; Bates, F. S.; Davis, K. P.; Lodge, T. P.; Klein, M. L.; DeVane, R. H.; Aqad, E.; Rosen, B. M.; Argintaru, A. O.; Sienkowska, M. J.; Rissanen, K.; Nummelin, S.; Ropponen, J. Self-assembly of Janus dendrimers into uniform dendrimersomes and other complex architectures. *Science* **2010**, *328*, 1009−1014. (b) Peterca, M.; Percec, V.; Leowanawat, P.; Bertin, A. Predicting the Size and Properties of Dendrimersomes from the Lamellar Structure of Their Amphiphilic Janus Dendrimers. *J. Am. Chem. Soc.* **2011**, *133*, 20507−20520. (c) Sherman, S. E.; Xiao, Q.; Percec, V. Mimicking complex biological membranes and their programmable glycan ligands with dendrimersomes and glycodendrimersomes. *Chem. Rev.* **2017**, *117*, 6538−6631. (d) Percec, V.; Leowanawat, P.; Sun, H.-J.; Kulikov, O.; Nusbaum, C. D.; Tran, T. M.; Bertin, A.; Wilson, D. A.; Peterca, M.; Zhang, S.; Kamat, N. P.; Vargo, K.; Moock, D.; Johnston, E. D.; Hammer, D. A.; Pochan, D. J.; Chen, Y.; Chabre, Y. M.; Shiao, T. C.; Bergeron-Brlek, M.; André, S.; Roy, R.; Gabius, H.-J.; Heiney, P. A. Modular synthesis of amphiphilic Janus glycodendrimers and their self-assembly into glycodendrimersomes and other complex architectures with bioactivity to biomedically relevant lectins. *J. Am. Chem. Soc.* **2013**, *135*, 9055−9077. (e) Xiao, Q.; Yadavalli, S. S.; Zhang, S.; Sherman, S. E.; Fiorin, E.; Silva, L.; da Wilson, D. A.; Hammer, D. A.; André, S.; Gabius, H.-J.; Klein, M. L.; Goulian, M.; Percec, V. Bioactive Cell-like Hybrids Coassembled from (Glyco)-Dendrimersomes with Bacterial Membranes. *Proc. Natl. Acad. Sci. U. S. A.* **2016**, *113*, E1134−E1141. (f) Yadavalli, S. S.; Xiao, Q.; Sherman, S. E.; Hasley, W. D.; Klein, M. L.; Goulian, M.; Percec, V. Bioactive Cell-like Hybrids from Dendrimersomes with a Human Cell Membrane and Its Components. *Proc. Natl. Acad. Sci. U. S. A.* **2019**, *116*, 744−752. (g) Rodriguez-Emmenegger, C.; Xiao, Q.; Kostina, N. Y.; Sherman, S. E.; Rahimi, K.; Partridge, B. E.; Li, S.; Sahoo, D.; Reveron Perez, A. M.; Buzzacchera, I.; Han, H.; Kerzner, M.; Malhotra, I.; Möller, M.; Wilson, C. J.; Good, M. C.; Goulian, M.; Baumgart, T.; Klein, M. L.; Percec, V. Encoding Biological Recognition in a Bicomponent Cell-Membrane Mimic. *Proc. Natl. Acad. Sci. U. S. A.* **2019**, *116*, 5376−5382. (h) Kostina, N. Yu; Rahimi, K.; Xiao, Q.; Haraszti, T.; Dedisch, S.; Spatz, J. P.; Schwaneberg, U.; Klein, M. L.; Percec, V.; Möller, M.; Rodriguez-Emmenegger, C. Membrane-Mimetic Dendrimersomes Engulf Living Bacteria via Endocytosis. *Nano Lett.* **2019**, *19*, 5732−5738. (i) Kostina, N. Y.; Söder, D.; Haraszti, T.; Xiao, Q.; Rahimi, K.; Partridge, B. E.; Klein, M. L.; Percec, V.; Rodriguez-Emmenegger, C. Enhanced Concanavalin A Binding to Preorganized Mannose Nanoarrays in Glycodendrimersomes Revealed Multivalent Interactions. *Angew. Chem., Int. Ed.* **2021**, *60*, 8352−8360.

(25) Zhang, D.; Atochina-Vasserman, E. N.; Maurya, D. S.; Huang, N.; Xiao, Q.; Ona, N.; Liu, M.; Shahnawaz, H.; Ni, H.; Kim, K.; Billingsley, M. M.; Pochan, D. J.; Mitchell, M. J.; Weissman, D.; Percec1, V. One-Component Multifunctional Sequence-Defined Ionizable Amphiphilic Janus Dendrimer Delivery Systems for mRNA. *J. Am. Chem. Soc.* **2021**, *143*, 12315−12327.

(26) Feng, X.; Burke, C. J.; Zhuo, M.; Guo, H.; Yang, K.; Reddy, A.; Prasad, I.; Ho, R.-M.; Avgeropoulos, A.; Grason, G. M.; Thomas, E. L. Seeing Mesoatomic Distortions in Soft-Matter Crystals of a Double-Gyroid Block Copolymer. *Nature* **2019**, *575*, 175−179.

(27) (a) Percec, V.; Cho, W.-D.; Mosier, P. E.; Ungar, G.; Yeardley, D. J. P. Structural Analysis of Cylindrical and Spherical Supramolecular Dendrimers Quantifies the Concept of Monodendron Shape Control by Generation Number. *J. Am. Chem. Soc.* **1998**, *120*, 11061−11070. (b) Percec, V.; Cho, W.-D.; Ungar, G. Increasing the Diameter of Cylindrical and Spherical Supramolecular Dendrimers by Decreasing the Solid Angle of Their Monodendrons via Periphery Functionalization. *J. Am. Chem. Soc.* **2000**, *122*, 10273−10281. (c) Percec, V.; Cho, W.-D.; Ungar, G.; Yeardley, D. J. P. Synthesis and Structural Analysis of Two Constitutional Isomeric Libraries of AB_2-Based Monodendrons and Supramolecular Dendrimers. *J. Am. Chem. Soc.* **2001**, *123*, 1302−1315. (d) Percec, V.; Mitchell, C. M.; Cho, W.-D.; Uchida, S.; Glodde, M.; Ungar, G.; Zeng, X.; Liu, Y.; Balagurusamy, V. S. K.; Heiney, P. A. Designing Libraries of First Generation AB_3 and AB_2 Self-Assembling Dendrons via the Primary Structure Generated from Combinations of $(AB)_Y$-AB_3 and $(AB)_Y$-AB_2 Building Blocks. *J. Am. Chem. Soc.* **2004**, *126*, 6078−6094. (e) Percec, V.; Holerca, M. N.; Nummelin, S.; Morrison, J. J.; Glodde, M.; Smidrkal, J.; Peterca, M.; Rosen, B. M.; Uchida, S.; Balagurusamy, V. S. K.; Sienkowska, M. J.; Heiney, P. A. Exploring and Expanding the Structural Diversity of Self-Assembling Dendrons through Combinations of AB, Constitutional Isomeric AB_2, and AB_3 Biphenyl-4-Methyl Ether Building Blocks. *Chem. - Eur. J.* **2006**, *12*, 6216−6241. (f) Percec, V.; Peterca, M.; Sienkowska, M. J.; Ilies, M. A.; Aqad, E.; Smidrkal, J.; Heiney, P. A. Synthesis and Retrostructural Analysis of Libraries of AB_3 and Constitutional Isomeric AB_2 Phenylpropyl Ether-Based Supramolecular Dendrimers. *J. Am. Chem. Soc.* **2006**, *128*, 3324−3334. (g) Percec, V.; Won, B. C.; Peterca, M.; Heiney, P. A. Expanding the Structural Diversity of Self-Assembling Dendrons and Supramolecular Dendrimers *via* Complex Building Blocks. *J. Am. Chem. Soc.* **2007**, *129*, 11265−11278. (h) Rosen, B. M.; Wilson, D. A.; Wilson, C. J.; Peterca, M.; Won, B. C.; Huang, C.; Lipski, L. R.; Zeng, X.; Ungar, G.; Heiney, P. A.; Percec, V. Predicting the Structure of Supramolecular Dendrimers *via* the Analysis of Libraries of AB_3 and Constitutional Isomeric AB_2 Biphenylpropyl Ether Self-Assembling Dendrons. *J. Am. Chem. Soc.* **2009**, *131*, 17500−17521.

(28) (a) Percec, V.; Bae, J.-Y.; Hill, D. H. Aryl Mesylates in Metal Catalyzed Homocoupling and Cross-Coupling Reactions. 2. Suzuki-Type Nickel-Catalyzed Cross-Coupling of Aryl Arenesulfonates and Aryl Mesylates with Arylboronic Acids. *J. Org. Chem.* **1995**, *60*, 1060−1065. (b) Rosen, B. M.; Quasdorf, K. W.; Wilson, D. A.; Zhang, N.; Resmerita, A.-M.; Garg, N. K.; Percec, V. Nickel-Catalyzed Cross-

https://doi.org/10.1021/jacs.1c08502
J. Am. Chem. Soc. 2021, 143, 17724−17743

Couplings Involving Carbon-Oxygen Bonds. *Chem. Rev.* **2011**, *111*, 1346−1416. (c) Percec, V.; Golding, G. M.; Smidrkal, J.; Weichold, O. $NiCl_2$(dppe)-Catalyzed Cross-Coupling of Aryl Mesylates, Arenesulfonates, and Halides with Arylboronic Acids. *J. Org. Chem.* **2004**, *69*, 3447−3452. (d) Rosen, B. M.; Huang, C.; Percec, V. Sequential Ni-Catalyzed Borylation and Cross-Coupling of Aryl Halides via in Situ Prepared Neopentylglycolborane. *Org. Lett.* **2008**, *10*, 2597−2600. (e) Wilson, D. A.; Wilson, C. J.; Moldoveanu, C.; Resmerita, A.-M.; Corcoran, P.; Hoang, L. M.; Rosen, B. M.; Percec, V. Neopentylglycolborylation of Aryl Mesylates and Tosylates Catalyzed by Ni-Based Mixed-Ligand Systems Activated with Zn. *J. Am. Chem. Soc.* **2010**, *132*, 1800−1801. (f) Leowanawat, P.; Zhang, N.; Resmerita, A.-M.; Rosen, B. M.; Percec, V. $Ni(COD)_2/PCy_3$ Catalyzed Cross-Coupling of Aryl and Heteroaryl Neopentylglycolboronates with Aryl and Heteroaryl Mesylates and Sulfamates in THF at Room Temperature. *J. Org. Chem.* **2011**, *76*, 9946−9955. (g) Zhang, N.; Hoffman, D. J.; Gutsche, N.; Gupta, J.; Percec, V. Comparison of Arylboron-Based Nucleophiles in Ni-Catalyzed Suzuki-Miyaura Cross-Coupling with Aryl Mesylates and Sulfamates. *J. Org. Chem.* **2012**, *77*, 5956−5964. (h) Jezorek, R. L.; Zhang, N.; Leowanawat, P.; Bunner, M. H.; Gutsche, N.; Pesti, A. K. R.; Olsen, J. T.; Percec, V. Air-Stable Nickel Precatalysts for Fast and Quantitative Cross-Coupling of Aryl Sulfamates with Aryl Neopentylglycolboronates at Room Temperature. *Org. Lett.* **2014**, *16*, 6326−6329. (i) Malineni, J.; Jezorek, R. L.; Zhang, N.; Percec, V. An Indefinitely Air-Stable σ-Ni^{II} Precatalyst for Quantitative Cross-Coupling of Unreactive Aryl Halides and Mesylates with Aryl Neopentylglycolboronates. *Synthesis* **2016**, *48*, 2795−2807. (j) Malineni, J.; Jezorek, R. L.; Zhang, N.; Percec, V. $Ni^{II}Cl$(1-Naphthyl)$(PCy_3)_2$, An Air-Stable σ-Ni^{II} Precatalyst for Quantitative Cross-Coupling of Aryl C-O Electrophiles with Aryl Neopentylglycolboronates. *Synthesis* **2016**, *48*, 2808−2815. (k) Hoffman, D. J. *Synthesis of Sterically Hindered ABn Dendritic Molecules via Nickel-Catalyzed Suzuki Cross-Coupling of Aryl Sulfonates and Aryl Boronic Acids and Esters*. MS Thesis, University of Pennsylvania, 2014.

(29) (a) Buzzacchera, I.; Xiao, Q.; Han, H.; Rahimi, K.; Li, S.; Kostina, N. Yu; Toebes, B. J.; Wilner, S. E.; Möller, M.; Rodriguez-Emmenegger, C.; Baumgart, T.; Wilson, D. A.; Wilson, C. J.; Klein, M. L.; Percec, V. Screening Libraries of Amphiphilic Janus Dendrimers Based on Natural Phenolic Acids to Discover Monodisperse Unilamellar Dendrimersomes. *Biomacromolecules* **2019**, *20*, 712−727. (b) Rice-Evans, C. A.; Miller, N. J.; Paganga, G. Structure-Antioxidant Activity Relationships of Flavonoids and Phenolic Acids. *Free Radical Biol. Med.* **1996**, *20*, 933−956. (c) Saibabu, V.; Fatima, Z.; Khan, L. A.; Hameed, S. Therapeutic Potential of Dietary Phenolic Acids. *Adv. Pharmacol. Sci.* **2015**, *2015*, 1. (d) Pandey, K. B.; Rizvi, S. I. Plant Polyphenols as Dietary Antioxidants in Human Health and Disease. *Oxid. Med. Cell. Longevity* **2009**, *2*, 270−278. (e) Natella, F.; Nardini, M.; Di Felice, M.; Scaccini, C. Benzoic and Cinnamic Acid Derivatives as Antioxidants: Structure-Activity Relation. *J. Agric. Food Chem.* **1999**, *47*, 1453−1459. (f) Mattila, P.; Hellström, J.; Törrönen, R. Phenolic Acids in Berries, Fruits, and Beverages. *J. Agric. Food Chem.* **2006**, *54*, 7193−7199. (g) Haminiuk, C. W. I.; Maciel, G. M.; Plata-Oviedo, M. S. V.; Peralta, R. M. Phenolic Compounds in Fruits-an Overview. *Int. J. Food Sci. Technol.* **2012**, *47*, 2023−2044. (h) Quideau, S.; Deffieux, D.; Douat-Casassus, C.; Pouységu, L. Plant Polyphenols: Chemical Properties, Biological Activities, and Synthesis. *Angew. Chem., Int. Ed.* **2011**, *50*, 586−621.

(30) Mohan, K. V. V. K.; Narender, N.; Srinivasu, P.; Kulkarni, S. J.; Raghavan, K. V. Novel Bromination Method for Anilines and Anisoles Using NH_4Br/H_2O_2 in CH_3COOH. *Synth. Commun.* **2004**, *34*, 2143−2152.

(31) Foley, J. W. *Chem. Abstr.* **1980**, *92*, 163705x (Synthesis (Polaroid Corp.), US-4182912).

(32) Percec, V.; Imam, M. R.; Peterca, M.; Leowanawat, P. Self-Organizable Vesicular Columns Assembled from Polymers Dendronized with Semifluorinated Janus Dendrimers Act As Reverse Thermal Actuators. *J. Am. Chem. Soc.* **2012**, *134*, 4408−4420.

(33) Vickery, E. H.; Pahler, L. F.; Eisenbraun, E. J. Selective O-Demethylation of Catechol Ethers. Comparison of Boron Tribromide and Iodotrimethylsilane. *J. Org. Chem.* **1979**, *44*, 4444−4446.

(34) (a) Cochran, W.; Crick, F. H. C.; Vand, V. The Structure of Synthetic Polypeptides. I. The Transform of Atoms on a Helix. *Acta Crystallogr.* **1952**, *5*, 581−586. (b) Peterca, M.; Percec, V.; Imam, M. R.; Leowanawat, P.; Morimitsu, K.; Heiney, P. A. Molecular Structure of Helical Supramolecular Dendrimers. *J. Am. Chem. Soc.* **2008**, *130*, 14840−14852.

(35) (a) Rosen, B. M.; Wilson, C. J.; Wilson, D. A.; Peterca, M.; Imam, M. R.; Percec, V. Dendron-Mediated Self-Assembly, Disassembly, and Self-Organization of Complex Systems. *Chem. Rev.* **2009**, *109*, 6275−6540. (b) Sun, H.-J.; Zhang, S.; Percec, V. From Structure to Function *via* Complex Supramolecular Dendrimer Systems. *Chem. Soc. Rev.* **2015**, *44*, 3900−3923.

(36) (a) Li, Y.; Lin, S.-T.; Goddard, W. A. Efficiency of Various Lattices from Hard Ball to Soft Ball: Theoretical Study of Thermodynamic Properties of Dendrimer Liquid Crystal from Atomistic Simulation. *J. Am. Chem. Soc.* **2004**, *126*, 1872−1885. (b) Ziherl, P.; Kamien, R. D. Maximizing Entropy by Minimizing Area: Towards a New Peinciple of Self-Organization. *J. Phys. Chem. B* **2001**, *105*, 10147−10158.

(37) (a) Sahoo, D.; Peterca, M.; Aqad, E.; Partridge, B. E.; Heiney, P. A.; Graf, R.; Spiess, H. W.; Zeng, X.; Percec, V. Hierarchical Self-Organization of Perylene Bisimides into Supramolecular Spheres and Periodic Arrays Thereof. *J. Am. Chem. Soc.* **2016**, *138*, 14798−14807. (b) Sahoo, D.; Imam, M. R.; Peterca, M.; Partridge, B. E.; Wilson, D. A.; Zeng, X.; Ungar, G.; Heiney, P. A.; Percec, V. Hierarchical Self-Organization of Chiral Columns from Chiral Supramolecular Spheres. *J. Am. Chem. Soc.* **2018**, *140*, 13478−13487. (c) Guerra, S.; Iehl, J.; Holler, M.; Peterca, M.; Wilson, D. A.; Partridge, B. E.; Zhang, S.; Deschenaux, R.; Nierengarten, J.-F.; Percec, V. Self-Organization of Dodeca-Dendronized Fullerene into Supramolecular Discs and Helical Columns Containing a Nanowire-Like Core. *Chem. Sci.* **2015**, *6*, 3393−3401.

(38) (a) Percec, V.; Dulcey, A. E.; Balagurusamy, V. S. K.; Miura, Y.; Smidrkal, J.; Peterca, M.; Nummelin, S.; Edlund, U.; Hudson, S. D.; Heiney, P. A.; Duan, H.; Magonov, S. N.; Vinogradov, S. A. Self-Assembly of Amphiphilic Dendritic Dipeptides into Helical Pores. *Nature* **2004**, *430*, 764−768. (b) Percec, V.; Dulcey, A. E.; Peterca, M.; Ilies, M.; Ladislaw, J.; Rosen, B. M.; Edlund, U.; Heiney, P. A. The Internal Structure of Helical Pores Self-Assembled from Dendritic Dipeptides Is Stereochemically Programmed and Allosterically Regulated. *Angew. Chem., Int. Ed.* **2005**, *44*, 6516−6521. (c) Percec, V.; Dulcey, A. E.; Peterca, M.; Ilies, M.; Sienkowska, M. J.; Heiney, P. A. Programming the Internal Structure and Stability of Helical Pores Self-Assembled from Dendritic Dipeptides via the Protective Groups of the Peptide. *J. Am. Chem. Soc.* **2005**, *127*, 17902−17909. (d) Percec, V.; Dulcey, A. E.; Peterca, M.; Ilies, M.; Nummelin, S.; Sienkowska, M. J.; Heiney, P. A. Principles of Self-Assembly of Helical Pores from Dendritic Dipeptides. *Proc. Natl. Acad. Sci. U. S. A.* **2006**, *103*, 2518−2523. (e) Peterca, M.; Percec, V.; Dulcey, A. E.; Nummelin, S.; Korey, S.; Ilies, M.; Heiney, P. A. Self-Assembly, Structural, and Retrostructural Analysis of Dendritic Dipeptide Pores Undergoing Reversible Circular to Elliptical Shape Change. *J. Am. Chem. Soc.* **2006**, *128*, 6713−6720. (f) Percec, V.; Dulcey, A. E.; Peterca, M.; Adelman, P.; Samant, R.; Balagurusamy, V. S. K.; Heiney, P. A. Helical Pores Self-Assembled from Homochiral Dendritic Dipeptides Based on l-Tyr and Nonpolar α-Amino Acids. *J. Am. Chem. Soc.* **2007**, *129*, 5992−6002. (g) Kaucher, M. S.; Peterca, M.; Dulcey, A. E.; Kim, A. J.; Vinogradov, S. A.; Hammer, D. A.; Heiney, P. A.; Percec, V. Selective Transport of Water Mediated by Porous Dendritic Dipeptides. *J. Am. Chem. Soc.* **2007**, *129*, 11698−11699. (h) Rosen, B. M.; Peterca, M.; Morimitsu, K.; Dulcey, A. E.; Leowanawat, P.; Resmerita, A.-M.; Imam, M. R.; Percec, V. Programming the Supramolecular Helical Polymerization of Dendritic Dipeptides via the Stereochemical Information of the Dipeptide. *J. Am. Chem. Soc.* **2011**, *133*, 5135−5151.

https://doi.org/10.1021/jacs.1c08502
J. Am. Chem. Soc. 2021, 143, 17724−17743

(39) Percec, V.; Dulcey, A.; Peterca, M.; Ilies, M.; Miura, Y.; Edlund, U.; Heiney, P. A. Helical Porous Protein Mimics Self-Assembled from Amphiphilic Dendritic Dipeptides. *Aust. J. Chem.* **2005**, *58*, 472−482.
(40) (a) Agre, P. Aquaporin Water Channels (Nobel Lecture). *Angew. Chem., Int. Ed.* **2004**, *43*, 4278−4290. (b) Preston, G.; Carroll, T.; Guggino, W.; Agre, P. Appearance of Water Channels in Xenopus Oocytes Expressing Red-Cell Chip28 Protein. *Science* **1992**, *256*, 385−387. (c) Walz, T.; Hirai, T.; Murata, K.; Heymann, J. B.; Mitsuoka, K.; Fujiyoshi, Y.; Smith, B. L.; Agre, P.; Engel, A. The Three-Dimensional Structure of Aquaporin-1. *Nature* **1997**, *387*, 624−627.
(41) Ungar, G.; Percec, V.; Holerca, M. N.; Johansson, G.; Heck, J. A. Heat-Shrinking Spherical and Columnar Supramolecular Dendrimers: Their Interconversion and Dependence of Their Shape on Molecular Taper Angle. *Chem. - Eur. J.* **2000**, *6*, 1258−1266.
(42) (a) Klug, A. From Macromolecules to Biological Assemblies (Nobel Lecture). *Angew. Chem., Int. Ed. Engl.* **1983**, *22*, 565−582. (b) Franklin, R. E.; Klug, A. The Splitting of Layer Lines in X-Ray Fibre Diagrams of Helical Structures: Application to Tobacco Mosaic Virus. *Acta Crystallogr.* **1955**, *8*, 777−780. (c) Franklin, R. E. Structure of Tobacco Mosaic Virus: Location of the Ribonucleic Acid in the Tobacco Mosaic Virus Particle. *Nature* **1956**, *177*, 928−930. (d) Franklin, R. E.; Klug, A. The Nature of the Helical Groove on the Tobacco Mosaic Virus Particle X-Ray Diffraction Studies. *Biochim. Biophys. Acta* **1956**, *19*, 403−416. (e) Percec, V.; Xiao, Q. The Legacy of Rosalind E. Franklin: Landmark Contributions to Two Nobel Prizes. *Chem.* **2021**, *7*, 529−536. (f) Percec, V.; Xiao, Q. Helical Self-Organizations and Emerging Functions in Architectures, Biological and Synthetic Macromolecules. *Bull. Chem. Soc. Jpn.* **2021**, *94*, 900−928. (g) Percec, V.; Xiao, Q. Helical Chirality of Supramolecular Columns and Spheres Self-Organizes Liquid Crystals, Crystals, and Quasicrystals. *Isr. J. Chem.* **2021**, DOI: 10.1002/ijch.202100057.
(43) Sahoo, D.; Peterca, M.; Aqad, E.; Partridge, B. E.; Heiney, P. A.; Graf, R.; Spiess, H. W.; Zeng, X.; Percec, V. Tetrahedral Arrangements of Perylene Bisimide Columns *via* Supramolecular Orientational Memory. *ACS Nano* **2017**, *11*, 983−991.
(44) (a) Percec, V.; Imam, M. R.; Peterca, M.; Wilson, D. A.; Graf, R.; Spiess, H. W.; Balagurusamy, V. S. K.; Heiney, P. A. Self-Assembly of Dendronized Triphenylenes into Helical Pyramidal Columns and Chiral Spheres. *J. Am. Chem. Soc.* **2009**, *131*, 7662−7677. (b) Percec, V.; Imam, M. R.; Peterca, M.; Wilson, D. A.; Heiney, P. A. Self-Assembly of Dendritic Crowns into Chiral Supramolecular Spheres. *J. Am. Chem. Soc.* **2009**, *131*, 1294−1304. (c) Percec, V.; Rudick, J. G.; Peterca, M.; Yurchenko, M. E.; Smidrkal, J.; Heiney, P. A. Supramolecular Structural Diversity among First-Generation Hybrid Dendrimers and Twin Dendrons. *Chem. - Eur. J.* **2008**, *14*, 3355−3362. (d) Peterca, M.; Imam, M. R.; Hudson, S. D.; Partridge, B. E.; Sahoo, D.; Heiney, P. A.; Klein, M. L.; Percec, V. Complex Arrangement of Orthogonal Nanoscale Columns *via* a Supramolecular Orientational Memory Effect. *ACS Nano* **2016**, *10*, 10480−10488. (e) Huang, N.; Imam, M. R.; Sienkowska, M. J.; Peterca, M.; Holerca, M. N.; Wilson, D. A.; Rosen, B. M.; Partridge, B. E.; Xiao, Q.; Percec, V. Supramolecular Spheres Assembled from Covalent and Supramolecular Dendritic Crowns Dictate the Supramolecular Orientational Memory Effect Mediated by Frank-Kasper Phases. *Giant* **2020**, *1*, 100001. (f) Huang, N.; Xiao, Q.; Peterca, M.; Zeng, X.; Percec, V. Self-Organisation of Rhombitruncated Cuboctahedral Hexagonal Columns from an Amphiphilic Janus Dendrimer. *Mol. Phys.* **2021**, No. e1902586.
(45) (a) Klug, A.; Finch, J. T.; Franklin, R. E. Structure of Turnip Yellow Mosaic Virus. *Nature* **1957**, *179*, 683−684. (b) Crick, F. H. C.; Watson, J. D. Structure of Small Viruses. *Nature* **1956**, *177*, 473−475. (c) Bernal, J. D.; Carlisle, C. H. Unit Cell Measurements of Wet and Dry Crystalline Type Yellow Mosaic Virus. *Nature* **1948**, *162*, 139−140. (d) Percec, V.; Holerca, M. N.; Uchida, S.; Cho, W.-D.; Ungar, G.; Lee, Y.; Yeardley, D. J. P. Exploring and Expanding the Three-Dimensional Structural Diversity of Supramolecular Dendrimers with the Aid of Libraries of Alkali Metals of their AB3 minidendritic Carboxylates. *Chem. - Eur. J.* **2002**, *8*, 1106−1117. (e) Percec, V.; Cho, W.-D.; Ungar, G.; Yeardley, D. J. P. Synthesis and NaOTf Mediated Self-Assembly of Monodendritic Crown Ethers. *Chem. - Eur. J.* **2002**, *8*, 2011−2025.
(46) (a) Kim, Y. H.; Webster, O. W. Water-Soluble Hyperbranchewd Polyphenylene: "A Unimolecular Micelle"? *J. Am. Chem. Soc.* **1990**, *112*, 4592−4593. (b) Kim, Y. H.; Webster, O. W. Hyperbranched Polyphenylenes. *Macromolecules* **1992**, *25*, 5561−5572. (c) Kim, Y. H. Hyperbranched Polymers 10 Years After. *J. Polym. Sci., Part A: Polym. Chem.* **1998**, *36*, 1685−1698. (d) Morgenroth, F.; Reuther, E.; Müllen, K. Polyphenylene Dendrimers: From Three-Dimensional to Two-Dimensional Structures. *Angew. Chem., Int. Ed. Engl.* **1997**, *36*, 631−634. (e) Nguyen, T.-T.-T.; Baumgarten, M.; Rouhanipour, A.; Rader, H.; Lieberwirth, I.; Müllen, K. Extending the Limits of Precision Polymer Synthesis: Giant Polyphenylene Dendrimers in the Megadalton Mass Range Approaching Structural Perfection. *J. Am. Chem. Soc.* **2013**, *135*, 4183−4186. (f) Hammer, B. A. G.; Müllen, K. Dimensional Evolution of Polyphenylenes: Expanding in all Directions. *Chem. Rev.* **2016**, *116*, 2103−2140.
(47) Tomalia, D. A.; Khanna, S. N. A Systematic Framework and Nanoperiodic Concept for Unifying Nanoscience: Hard/Soft Nanoelements, Superatoms, Meta-Atoms, New Emerging Properties, Periodic Property Patterns, and Predictive Mendeleev-like Nanoperiodic Tables. *Chem. Rev.* **2016**, *116*, 2705−2774.

https://doi.org/10.1021/jacs.1c08502
J. Am. Chem. Soc. 2021, 143, 17724−17743